



# An innovative methodology for the adjustable use of energy line angle for susceptibility mapping by using cone propagation approach

**Abstract** Rockfall frequently occurs in the mountainous areas and threatens structures such as settlement areas, transportation lines, and agricultural field. The empirical approaches for rockfall mapping have been an attractive research topic in rock mechanics in the recent years, because producing rockfall maps of large areas by using the deterministic and the probabilistic analysis seems difficult due to the necessity of numerous inputs. The cone propagation approach is preferred as a practical tool particularly in the regional scale. The digital elevation model (DEM) of a region prone to rockfall is used for determination of possible propagation zones based on a simple geometric rule known as the energy line angle (reach angle). As a new term,  $ELA_{max\_stop}$  was defined to represent the energy line angle that extends to the border of the propagation zone as the maximum run-out distance that is obtained from application of the cone approach to all points (pixels) in source area. The angle denoted as  $\alpha$  refers to the threshold slope angle of the steep areas utilized to identify potential source areas by using DEM. Conceptually, the fallen rock blocks within a rockfall-prone region stop within the cone propagation zone, which is bounded by the energy line angles  $\alpha$  and  $ELA_{max\_stop}$ . While the value of  $\alpha$  is susceptible to the resolution of DEM,  $ELA_{max\_stop}$ , which exhibits a wide angle range as documented in the literature, is controlled by rock block features together with slope surface properties of the propagation zone. Due to the variability of  $ELA_{max\_stop}$  and  $\alpha$  depending on the studied region and the resolution of the DEM, the boundary value of the energy line angles between different susceptibility classes need to be adjusted by considering  $\alpha$  and  $ELA_{max\_stop}$ . By adopting the cone propagation approach to enable adjustable use of energy line angles for rockfall susceptibility mapping, a series of graphical presentations was prepared. These graphical presentations allowed for the prediction of energy line angles corresponding to various rockfall susceptibility classes including very low, low, medium, high, and very high. In addition to the graphical presentations, a series of practical equations were derived for the same purpose. In the final part of the study, a new rating system, namely the run-out distance rating (RDR), was introduced for the preliminary determination of  $ELA_{max\_stop}$ . Due to the empirical structure of the methodology, the suggested supportive approach to the practitioners for determining  $ELA_{max\_stop}$  should be considered as an initial step that opens to improvement. The proposed methodology in this study was implemented in the regions of Kargabedir Hill and Sivrihisar residential areas in Turkey to prepare rockfall susceptibility maps.

**Keywords** Rockfall · DEM · Source area map · Cone propagation approach · Energy line angle · Susceptibility map

## Introduction

Rockfall is defined as a type of instability in which rock blocks are released from jointed rock masses on steep slopes and move at high speed down along the slope (Varnes 1978). Rockfalls are usually triggered by various climatic and biological changes or external forces such as earthquakes. The released rock block from a source area moves downward on the slope surface until its kinetic energy reduces to zero. As known, it is possible to consider rockfall susceptibility assessment methods under two sub-groups as 2D or three-dimensional (3D) deterministic or probabilistic analyses and the empirical approaches. Deterministic or probabilistic rockfall analyses are based on the principles of fundamental physics.

Corominas et al. (2005) performed a study about the evaluation of the rockfall risk at the Solà d'Andorra slope (Andorra Principality) by considering the implementation of risk mitigation works. Rockfall susceptibility map of Gunung Kelir in Java was based on the velocity of rockfall movement studied by Samodra et al. (2016). For this aim, the researchers performed back analysis of rockfall by using RockFall Analyst developed by Lan et al. (2007). Antoniou and Efthimios Lekkas (2010) performed a study about the preparation of the rockfall susceptibility map for Athinios port, Santorini Island in Greece. For this aim, the researchers identified three zones having different degrees of susceptibility such as low, medium, and high by taking into account human activities. For determination of maximum travel, distance (run-out distance) along each profile was determined empirically by using reach angle. Farvacque et al. (2022) performed a study for estimation of rockfall frequency by using a new procedure. Field analysis of rockfall deposits in mitigation structures and growth disturbances in tree-ring series with 3D was taken into consideration by Farvacque et al. (2022). Then, the researchers proposed a process-based rockfall modeling for predicting rockfall frequencies of individual cliff compartments.

On the other hand, recent technologies such as terrestrial laser scanning (TLS) or light detection and ranging (LiDAR) provide significant advantages for monitoring slope movements and deformations, and also early warning systems. A well-documented review about the use of LiDAR in landslide investigations was presented by Jaboyedoff et al. (2012). Williams et al. (2019) focused on the importance of monitoring intervals for rockfall magnitude-frequency estimation. By using LiDAR technology, Williams et al. (2019) aimed to detect small rockfall, which, in sum, contributes significantly to overall volume loss from rock slopes in this setting (Williams et al. 2019). Kromer et al. (2018) assessed potential failure time through the application of inverse velocity methods. Based on monitoring of 90 rockfalls, the percentage of the detecting pre-failure deformation

was obtained as 70% (Kromer et al. 2018). Farmakis et al. (2020) performed a study for automated analysis and characterization of jointed rock mass in 3D space at the Santorini Island in Greece. For this aim, the LiDAR technology and the conventional methods were used together for the data comparisons. Farmakis et al. (2020) aimed to investigate the detailed high-resolution rock mass characterization, in terms of the predisposing factors involved in rockfall susceptibility assessment as well the possible failures along the slopes. A recent study was performed by Farmakis et al. (2022) about rockfall detection by using LiDAR and deep learning. As a conclusion, Farmakis et al. (2022) emphasized that the use of LiDAR monitoring and deep learning is challenging to achieve generalization in rockfall detection, and site-specific training of the proposed deep learning architecture can lead to high-level performance and support further advancements in rockfall risk management.

In addition to innovative techniques such LiDAR used for rockfall assessments, the deterministic and the empirical assessments of rockfall are still inevitable. In deterministic rockfall analysis, the most critical parameter controlling the motion of the rock block is the coefficients of restitution between rock block and slope surface. The definition for the coefficient of restitution ( $R$ ) is known as the ratio of the energies or velocities of the rock block that hits the slope surface before and after the impacts. It is divided into two components as the tangential ( $R_t$ ) and the normal ( $R_n$ ) coefficient of restitution depending on the direction of motion at the point of impact. However, the selection of  $R_t$  and  $R_n$  is the most critical task for the successful rockfall analysis. In addition to some recommendations that are available in the literature for the selection of  $R_n$  and  $R_t$  values according to the surface properties of slope,  $R_n$  and  $R_t$  values can also be determined by back analysis of the rock blocks released from the source area. In the deterministic and probabilistic analyses performed by using reliable inputs, it is possible to predict the trajectory of the falling rock block and also to determine its velocity and energy along the trajectory. Thus, these analyses can provide very useful information especially for the design of protection structures against rockfall. However, in deterministic and probabilistic rockfall analysis approaches, many physical and mechanical parameters related to both the slope surface and the rock block are used as inputs. Therefore, the results are highly susceptible to the accuracy of input parameters such as coefficients of restitutions ( $R_n$  and  $R_t$ ), initial velocity of the rock blocks, block shapes, and friction coefficient between the rock block and the surface. Although the rockfall mechanism is quite simple to explain by using basic physical principles, their practical value in the preparation of rockfall maps especially at regional scale may be relatively insufficient. Larcher et al. (2012) stated that “particularly at a regional scale, because the most well-known methods are applicable only in small territories and generally along pre-defined fall profiles that do not contemplate lateral diffusion.” Due to the difficulties encountered in the determination of the numerous input parameters used in the deterministic and the probabilistic rockfall analysis approaches, empirical approaches, which estimate run-out distances by using determination of source areas, come forward (Larcher et al. 2012). On the other hand, the most important advantage of regional-scale analyses by using empirical approaches can be mainly stated that these studies are cost-effective methodologies to be applied over wide territories and do not necessitate numerous input data and could lead anyhow to reliable results.

The cone propagation approach proposed by Jabodeyoff and Labiouse (2003) is widely preferred in order to define the susceptibility application of large areas to rockfall, since it can be run with simple inputs. This practical approach is based on the principle of determining the propagation zone on digital elevation model (DEM) of the field. The rockfall source area map and DEM are sufficient for the use of the cone propagation approach.

Kalender (2017) performed the well-inventoried studies in two rockfall-prone regions, namely Kargabedir Hill and Sivrihisar residential area in Turkey during her PhD thesis. A study for evaluation of rockfall susceptibility of Kargabedir Hill region by the cone propagation approach using unmanned aerial vehicle (UAV) images was published by Kalender and Sonmez (2019). The authors especially focused on the measurement of dimensions of the rock blocks from the UAV images, but cone propagation zones were also drawn on map by using energy line angles from 20 to 45° with 5° increments. In other words, Kalender and Sonmez (2019) studied the rockfall map of Kargabedir Hill region by using the cone propagation approach for arbitrarily selected energy line angles from 20 to 45° with 5° increments. As known, the maximum run-out distance refers to the maximum distance from the source area that fallen rock blocks can reach within a region prone to rockfall. A new term called as  $ELA_{max\_stop}$  was defined to represent the energy line angle that extends to the border of the propagation zone as the maximum run-out distance that is obtained from application of the cone approach to all points (pixels) in source area. The angle denoted as  $\alpha$  is a threshold slope angle of the steep areas to be used for identifying potential rockfall source areas by using DEM. Conceptually, all fallen rock blocks in a rockfall-prone area stop within the cone propagation zone. The cone propagation zone is bounded by the border of the source area produced by using the threshold angle ( $\alpha$ ) on DEM and the maximum run-out border of the propagation zone obtained from the application of cone approach to all points in the source area by using  $ELA_{max\_stop}$ . In other words,  $\alpha$  and  $ELA_{max\_stop}$  are two important energy line angle values to be considered as two extreme values in the cone propagation approach. The value of  $ELA_{max\_stop}$  which exhibits a wide angle range as documented in the literature, is influenced by the rock block features and slope surface properties of the propagation zone. On the other hand, the value of  $\alpha$  is susceptible to the resolution of DEM. Due to the variability of both  $ELA_{max\_stop}$  and  $\alpha$  depending on the site-specific properties of the studied region and the resolution of DEM, the boundary energy line angles between different susceptibility classes to be used rockfall susceptibility mapping need to be adjusted depending on the values of  $\alpha$  and  $ELA_{max\_stop}$ . For this aim, a series of graphical presentations were prepared to be selected depending on the values of  $\alpha$  and  $ELA_{max\_stop}$ . These graphical presentations facilitated the prediction of energy line angles corresponding to the degree of rockfall susceptibility classes including very low, low, medium, high, and very high. By using the innovative approach, it is possible to determine the energy line angles corresponding to rockfall susceptibility classes by the site-specific assessments for any rockfall-prone region. In other words, the values of energy line angles corresponding to rockfall susceptibility classes such as very low, low, moderate, high, and very high can be determined to be specific to the studied region. In addition, S-shaped curves on the graphical representations were defined by a series of equations for the practical use of the same purpose especially in the computer medium.

Ritchie (1963) stated that the run-out distance of a fallen rock block is controlled by the rockfall source area (starting point), block shape and geometry, surface topography, and mechanical properties of the rock mass. Therefore, determining the applicable  $ELA_{max\_stop}$  at least as a preliminary value for a studied region necessitates adopting a user-controlled new approach. The main subject of the study is the innovative approach for the use of adjustable energy line angle for producing a rockfall susceptibility map. However, the maximum run-out distance rating (RDR) system was introduced as an initial attempt for the preliminary determination of  $ELA_{max\_stop}$  in the final part of the study. The determined value of  $ELA_{max\_stop}$  by using the proposed RDR system should not be perceived as an indispensable value; however, it can be considered as a preliminary default value open to user control. The supportive approach for determining  $ELA_{max\_stop}$  should be regarded as a modest start-in and should remain open to improvement.

The proposed innovative methodology was implemented in the regions of Kargabedir Hill and Sivrihisar residential areas in Turkey, resulting in the preparation of accurate rockfall susceptibility maps.

## Methodology

### An introductory overview of the Conefall propagation method

The energy line angle (ELA) defined by Heim (1932) is the fundamental data for the Conefall approach. The ELA is also referred to in the literature by different names such as the Fahrbuschung angle or the reach angle. The energy line angle is expressed by the slope of the linear line between the releasing and the stopping points of a fallen rock block (Fig. 1c). In addition, the length of this line is defined as the run-out distance that a rock block can reach the furthest point to stop. The value of energy line angle and run-out distance are inversely related to each other, and as run-out distance increases, the value of energy line angle decreases. The fallen rock block moves downward along a trajectory depending on the ELA, and a potential area is affected along the trajectory. The area which has the potential to be affected by the rockfall event is defined as the propagation zone.

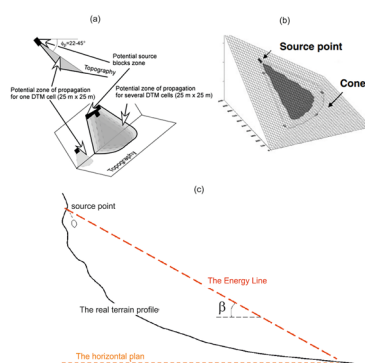


**Fig. 1** a Principle of the cone method, with cells as source areas. b Illustration of the areas endangered by rockfalls starting from a source point, using cone slopes of 35° and 40° (from the Conefall user's guide). c Energy line angle concept (modified from Larcher et al. 2012)

The empirical approach known as the Conefall method was introduced to the literature by Jaboyedoff and Labiouse (2011). As given in detail by Jaboyedoff and Labiouse (2011), for the application of the cone propagation approach, a vertical cone whose apex point is fixed to a source cell in the digital elevation model is drawn with the angle determined according to the concepts of energy line angle (Fig. 1a, b). The area of the slope topography under this vertical cone is identified as the rockfall spreading zone. The number of potential exposures to rockfall in each cell in the propagation zone can be obtained, as well as determination of the border of propagation zones, velocity, and kinetic energy distributions with the Conefall v1.0 free software developed by Jaboyedoff and Labiouse (2011). The output files of the Conefall v1.0 software are in ASCII format and can be easily transformed into maps by using any available Geographic Information System (GIS) software.

Basically, a rockfall event is possible only when there are potential rockfall source areas in the studied region. For this reason, determination of rockfall source areas is the first step for the rockfall mapping. Another well-known reality for the rockfall event is that the potential source areas should have steep topography. The mapping of potential source areas by only conventionally field studies requires a highly time-consuming and difficult process at regional scale. To overcome this difficulty by using a simple computer operation, the areas above a certain steep slope angle depending on the resolution of the slope map can be identified as the potential rockfall source areas. In other words, the areas above a certain steep slope on the slope maps to be obtained from the DEM can be considered as the potential rockfall source areas. The fundamental consideration for this purpose is the resolution of the DEM, as it strongly influences the representation of in situ topography in the GIS-based computer medium. It may be briefly stated that the slope map obtained from a high-resolution DEM will be closer to the in situ topographical conditions. Larcher et al. (2012) proposed the following simple equation for calculation of the threshold value of the slope angle depending on the resolution of DEM for identifying the potential source areas:

$$\alpha = 55(\text{RES})^{-0.075} \quad (1)$$

where  $\alpha$  is the threshold slope angle (in degrees) for identifying the potential rockfall source areas and RES is the resolution of DEM (in meters). It should be underlined that the areas having a slope value higher than  $\alpha$  are only defined as the potential rockfall source areas. Therefore, the areas identified by using the simple equation given in Eq. 1 should be taken into consideration as a preliminary step for identifying rockfall source areas. The additional efforts for the validation in the field may be needed for identifying more precise borders of rockfall source areas by including or excluding some areas.

## Field studies

The data belonging to some researchers regarding the percentage of rock blocks stopped in the area bordered by a studied energy line angle is given as a graphical presentation in Fig. 2. An S-shaped curvilinear relationship that provides the best possible distribution has been defined by ignoring data which belong to Toppe (1987). The S-shaped cumulative normal

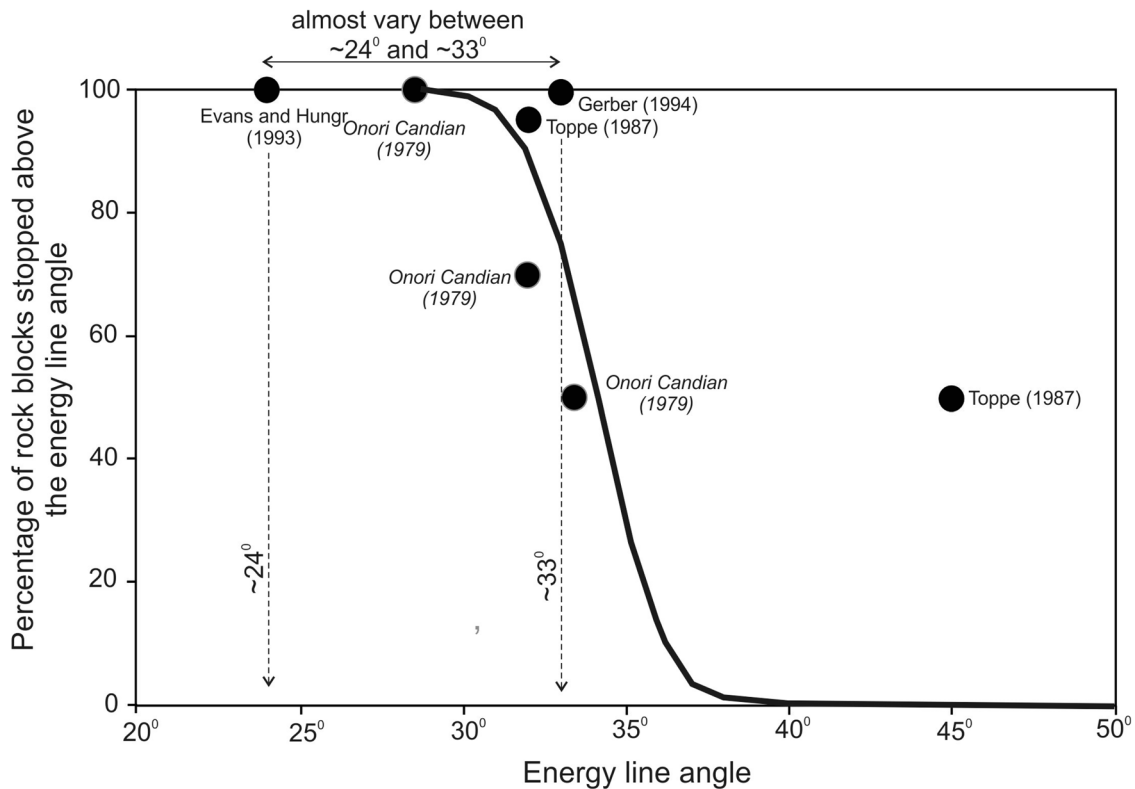


**Fig. 2** Relationships between energy line angles and block distributions according to various authors. The curve is a fitting of all results by ignoring the point from Toppe (1987) (modified from Jaboyedoff and Labiouse 2011)

statistical distribution curve may be acceptable for the general shape of the curvilinear relationship due to the nature of rockfall event in the propagation zone. Therefore, to produce rockfall susceptibility maps, it can be stated that the statistical distributions of the fallen rock blocks on the slope surface is important in terms of producing propagation zones having different degrees of susceptibility. By considering the importance of the statistical distribution between the fallen rock block proportion and energy line angle values within the propagation zone, it was investigated statistically in the studied areas before the development of methodology for the adjustable use of energy line angle for susceptibility mapping by using the cone propagation approach. For this reason, first of all, the locations and dimensions (width, length, and height) of the fallen rock blocks on the slope surfaces in the studied areas were recorded. Afterward, the rockfall source area maps for the studied areas were prepared by using a DEM. The field studies were carried out by Kalender (2017) in Kargabedir Hill and Sivrihisar residential areas. Although the PhD thesis performed by Kalender (2017) is unpublished, a study for evaluation of rockfall susceptibility of Kargabedir Hill region by the cone propagation approach using UAV images was published by Kalender and Sonmez (2019).

#### Kargabedir Hill rockfall area

Kalender (2017) and Kalender and Sonmez (2019) presented the well-inventoried field studies carried out in the Kargabedir Hill rockfall area as follows.

One of the studies including geology of Kargabedir Hill and close vicinity was performed by Rojay and Suzen (1997). Kargabedir Hill is a volcanic jointed rock mass and located within the borders of Ballıkuyumcu Village, Ankara, Turkey (Fig. 3). In addition to the presence of some houses at the foot of the hill, the road connecting Ankara and Eskişehir passes through here. Kargabedir Hill is located at about 950 m elevation and was formed by volcanic activity. Due to the steep topography of the rockfall source areas, discontinuity orientations could not be investigated by the suggested procedures of ISRM such as the scanline surveys or the window mapping. On the other hand, as is well known, the shape of blocks is one of the important properties which affects the maximum run-out distance of the fallen rock blocks. By considering this fact, to identify general block shapes such as equal dimensional, columnar, or flat, height, width, and length of the fallen rock block on the slope surface were measured. The histogram graphs with their average ratios of width to length, height to length, and width to height of 0.74, 0.70, and 1.12, respectively, are given in Fig. 4. The values of these three-dimensional ratios equal to 1 represent that the shape of the rock block can be accepted as equidimensional. Equidimensional rock block can also be defined as a measure of the block to be placed in a cubic volume in which the fallen block is touching all its surfaces as much as possible. Therefore, the measure of three-dimensional ratios of the fallen rock block close to 1 can be used as an indicator of equidimensionality of a rock block. After these explanations, it may be concluded that the block shapes of the fallen rock blocks observed in the Kargabedir Hill rockfall area can be assumed as close to equidimensional rock block shape.





**Fig. 3** Location map of the studied areas on the active fault map of Turkey (from Emre et al. 2013) overlaid on Google Earth view

In the Kargabedir Hill rockfall area, the fallen rock blocks reach a maximum run-out distance of about 200 m laterally from the rockfall source area. The slope surface in the Kargabedir Hill rockfall area is generally covered by talus, and the semi-buried large rock blocks are also observed especially in the accumulation zone. The talus consists of rock pieces and/or blocks of different sizes mixed with the fine-grained soil. The fallen rock blocks are generally semi-angular, and the slope surface is smooth. However, the fallen semi-buried rock blocks in the talus create the protrusions (tortuosity) on the smooth slope surface (Fig. 5a). In addition to the field studies, high-resolution aerial photographs of the area were taken by using a UAV (drone) to produce a high-resolution DEM of the area. Totally 695 photos with 12-megapixel resolution were taken from the area of 0.703 km<sup>2</sup>, enclosing the Kargabedir Hill. A digital elevation model with a resolution of 40 × 40 cm and an orthorectified aerial photograph with a resolution of 5 × 5 cm were created with the computer program

Agisoft PhotoScan (2017, version 1.3.0 3772) by using the 343 of 695 photographs by sorting out the overlapping ones. The dimensions and locations of 463 fallen rock blocks which reflect the overall block distribution as much as possible were measured by using both in situ and orthorectified aerial photograph produced from the 695 photos with 12-megapixel resolution taken by a UAV (drone) (Fig. 6a). The volumetric distribution histogram of the measured blocks is presented in Fig. 6b. It is seen in Fig. 6b that the volumetric distribution of rock blocks is similar to the negative exponential distribution. In another words, depending on the increase in the volume of the rock block, its frequency in the field decreases. Although a 40 × 40 cm high-resolution digital elevation model was prepared, by considering computing performance of the Conefall v1.0 program, the resolution of the DEM was reduced to 2 × 2 m. The threshold slope angle for rockfall source area by using RES = 2 m was determined as  $\alpha = 52^\circ$  by using Eq. 1 which is a practical empirical relation for determination of a threshold slope

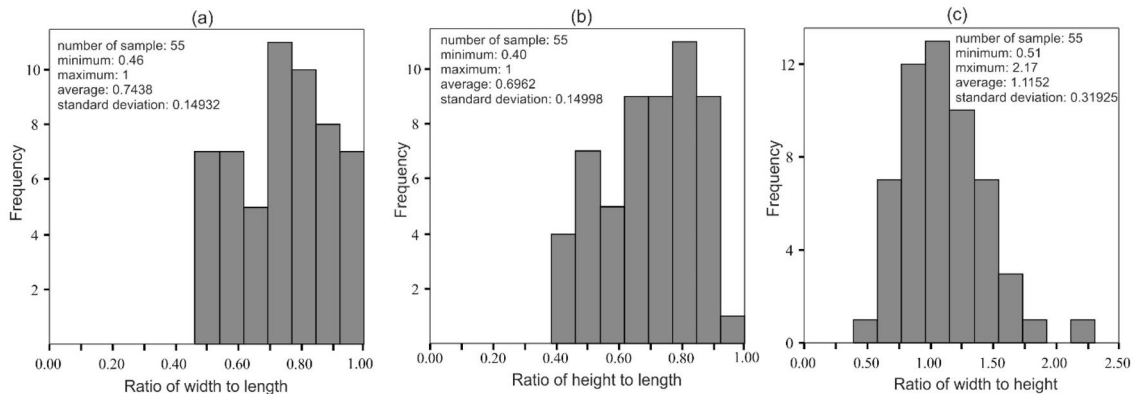


**Fig. 4** The histogram graphs for the ratio of blocks' dimensions with their statistical summary for the Kargabedir Hill rockfall area. **a** Width to length. **b** Height to length. **c** Width to length (from Kalender (2017) and Kalender and Sonmez (2019))



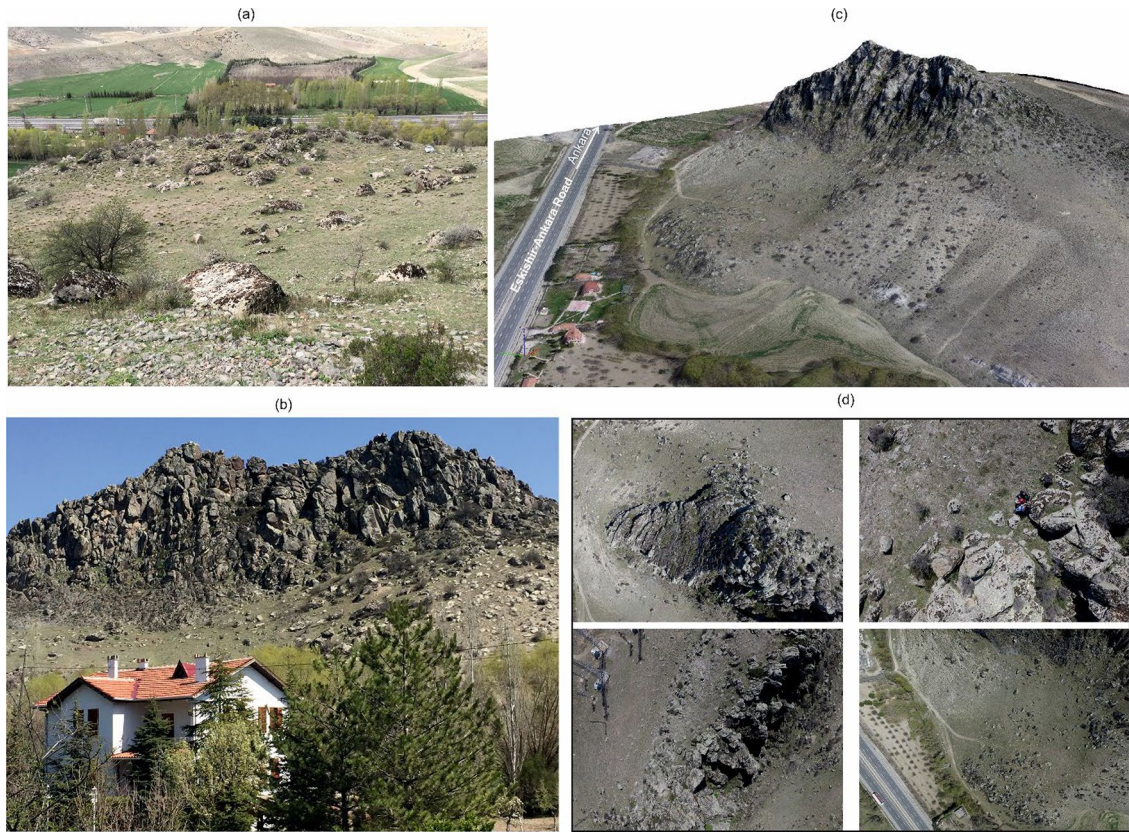


**Fig. 5** **a** Previously fallen and semi-buried rock blocks on the smooth talus slope surface. **b** View of the Kargabedir Hill from the Eskisehir-Ankara road. **c** Three-dimensional real view obtained from 12-megapixel aerial photos of Kargabedir Hill. **d** The close view examples on the orthorectified aerial photograph produced by using 12-megapixel aerial photos of Kargabedir Hill (modified from Kalender (2017) and Kalender and Sonmez (2019))

angle to be considered for identifying the potential source areas in terms of rockfall assessments. The areas having a slope above the threshold slope value were extracted as the rockfall potential source

area. However, the rockfall potential source areas obtained from Eq. 1 should be controlled whether whole identified source areas are reliable for the possible rockfall source areas in the Kargabedir Hill

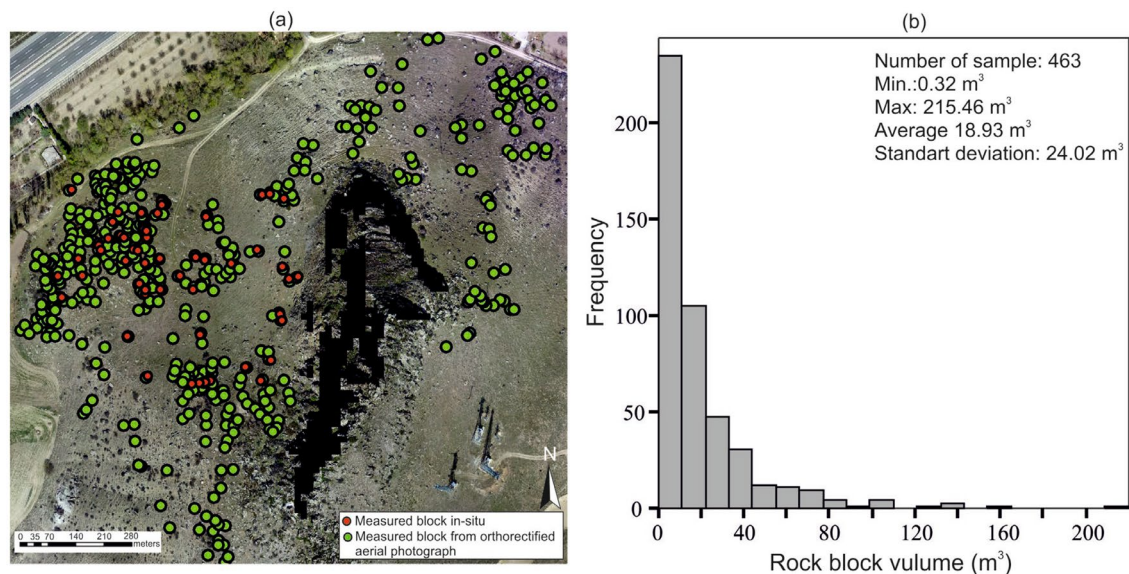


**Fig. 6** **a** Locations of the measured rock blocks on the orthorectified aerial photograph. **b** The volume distribution histogram graph of 463 fallen rock blocks for the Kargabedir Hill rockfall area (from Kalender (2017) and Kalender and Sonmez (2019))



rockfall area. For Kargabedir rockfall region, a highly compatible result has been observed between the rockfall potential source areas in the orthorectified views and the areas were identified by using threshold slope angle ( $\alpha$ ). Therefore, the rockfall potential source areas identified by considering Eq. 1 were preserved as is.

Kargabedir Hill case resembles an almost upright cone with an aspect of slope surfaces to all dip directions from 0 to 360°. By considering this morphological property, “No limit angle” option was used in the Conefall v1.0 (Quanterra, 2003). Therefore, a user-controlled dip direction for expectance of rockfall occurrence and dip aperture

range for Kargabedir Hill rockfall case were not taken into consideration. The cone propagation zones by considering the energy line angle values corresponding to 5° increments from 20 to 45° and the propagation zones were identified by using the Conefall v1.0 program. Afterward, the locations of 463 inventoried boulders were signed on the propagation zone map overlaid on the orthorectified aerial image by using ArcGIS v9.1 (ESRI, 2007) program (Fig. 7). The percentage of the fallen rock blocks within the propagation zones, which were determined based on the values of ELA, by considering the fallen rock blocks was calculated in the ArcGIS v9.1 program (Table 1).

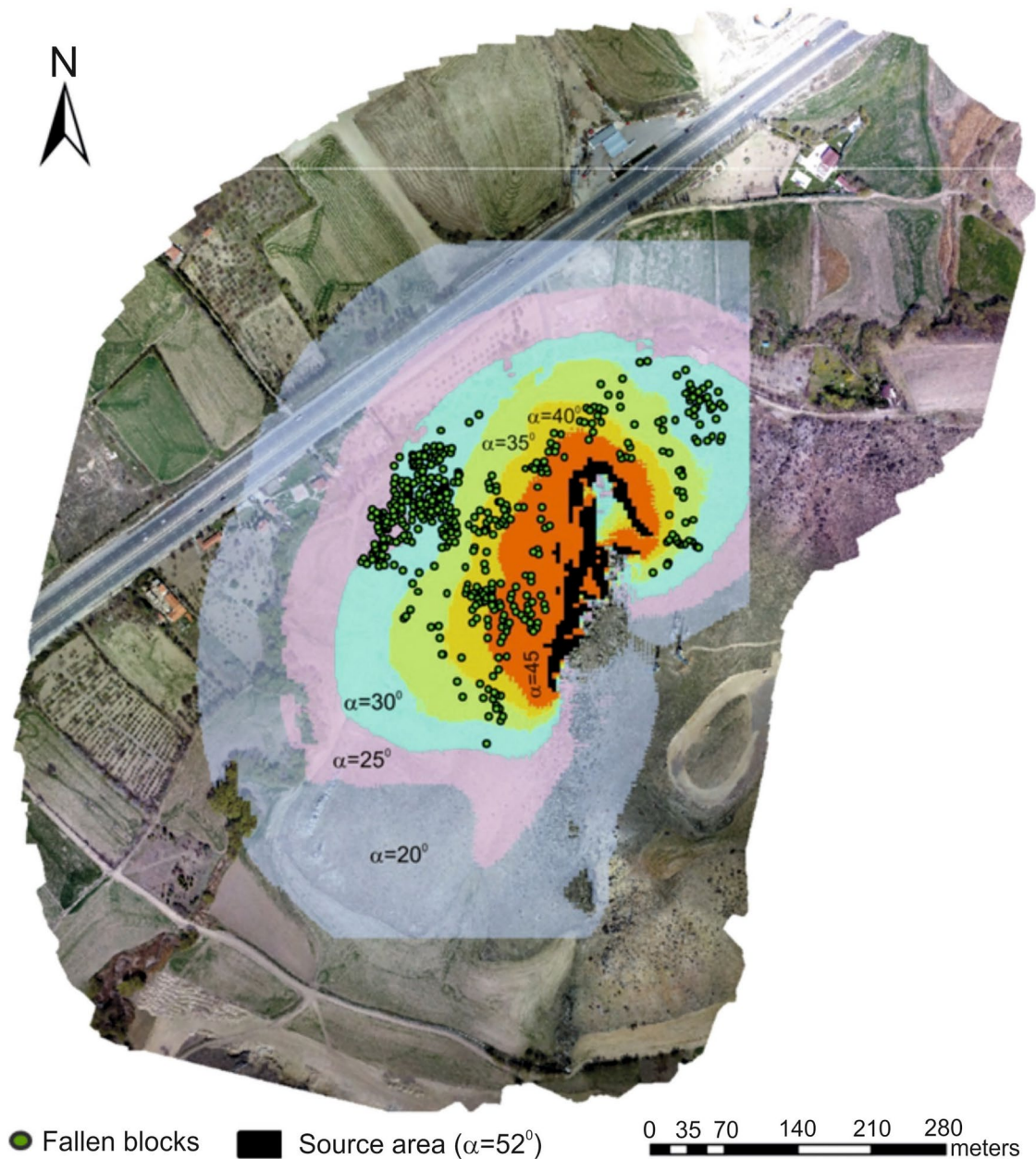


**Fig. 7** Propagation zones for different energy line angle values in the Kargabedir Hill rockfall region (from Kalender (2017) and Kalender and Sonmez (2019))

**Table 1** The percentage of the rock blocks within the propagation zones for the Kargabedir Hill rockfall area (from Kalender (2017) and Kalender and Sonmez (2019))

Energy line angle (°)	Rock block percentage (%)
20	100
25	100
30	88.6
35	48.8
40	34.3
45	25.3

#### Sivrihisar residential rockfall area

The granodiorite steep rock mass exposure, which frames the Sivrihisar residential area in Eskisehir Province, was selected as a second case (see Fig. 3). Kalender (2017) presented the well-inventoried field studies carried out in the Sivrihisar residential rockfall area as follows.

The information about the geology of Sivrihisar residential area and its close vicinity was available in the study performed by Yılmaz (2003). The jointed granodiorite rock mass extends over a wide area

in the form of an arc on the northwest-southeast line in the north-east of the district (Fig. 8). The fallen blocks, which had been released from the jointed granodiorite mass, move along the slope up to the walls of the settlements and reached 700 m laterally away. The slope surface, on which the blocks are spread, is covered with talus and has a smooth surface characteristic. The fallen rock blocks have different sizes, and some of them are semi-buried rock blocks within the talus. The angularity of the blocks varies between sub-rounded and sub-angular in general. Because of the steep topography of the source areas, discontinuity properties could not be investigated by the suggested procedures of ISRM such as scanline surveys and window mapping. However, the dimensions and locations of the 256 fallen blocks were measured during field studies in the Sivrihisar residential rockfall area. The histogram graphs with their average values of width to length, height to length, and width to height are given as 0.63, 0.52, and 1.41, respectively, in Fig. 9a. By considering general distribution of the calculated dimensional ratios between 0.5 and 1.5, it is possible to say that the blocks in most parts of the area are somewhat equidimensional. When the average values of the calculated ratios were compared with the same values belonging to the Kargabedir Hill rockfall area, it can be said that the rock blocks of the Kargabedir Hill rockfall area are slightly closer to equidimensionality. The volume distribution histogram of these blocks is given in Fig. 9b.

Unlike the Kargabedir Hill rockfall area, due to the large size of the area, a high-resolution digital elevation model could not be



**Fig. 8** **a** View of the granodiorite rock mass encircling the Sivrihisar residential area in Google Earth image. **b–d** Views from Sivrihisar residential area and the encircled granodiorite rock mass (modified from Kalender 2017)



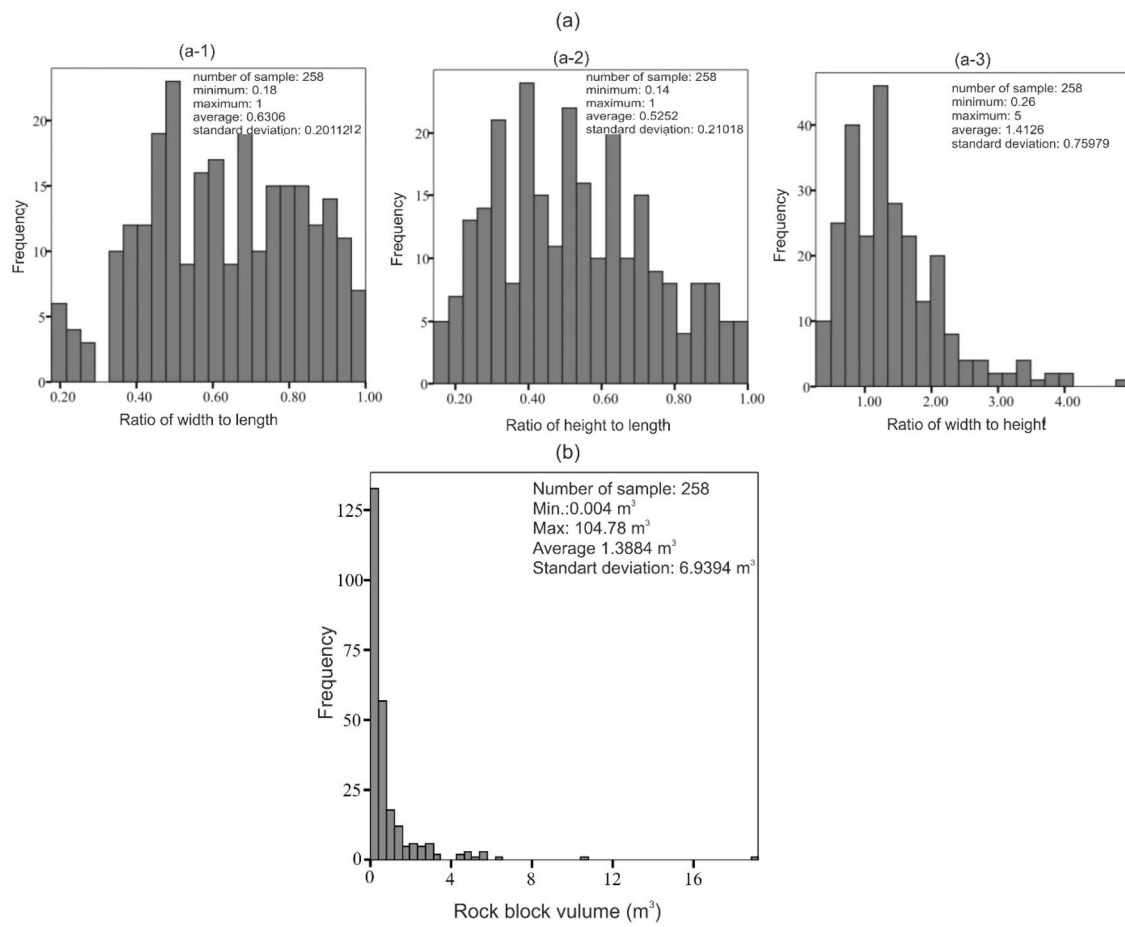


**Fig. 9** **a** The histogram graphs for ratio of blocks' dimensions with their statistical summary for the Sivrihisar residential rockfall area (a-1) width to length, (a-2) height to length, and (a-3) width to length. **b** The volume distribution histogram graph for the Sivrihisar residential rockfall area (from Kalender 2017)

processed by using aerial photos to be taken from the Sivrihisar residential area. Therefore, a digital elevation model having  $10 \times 10$  m resolution was produced from the 1/25,000-scale topographic map and used in the analysis. On the other hand, the use of low-resolution DEM of the second case provides an attempt to the use of the innovative methodology having a DEM with low resolution. The threshold slope angle ( $\alpha$ ) was obtained as  $46^\circ$  from Eq. 1 by using 10 m DEM resolution. However, the areas having a slope higher than  $\alpha = 46^\circ$  were insufficient to cover the whole rockfall source areas when it was compared with both rock exposures in situ and on Google Earth image of the studied area. Therefore, it is necessary to reduce the value of  $\alpha$  to enlarge areas to cover the whole rockfall potential source areas. The value of  $\alpha$  was gradually reduced by user control. The value of  $\alpha$ , which was about equal to  $35^\circ$ , was observed as a sufficient threshold slope angle value to cover almost whole rockfall potential source areas for the Sivrihisar residential rockfall area as the second case. It should be underlined that the use of Eq. 1 is not a straightforward process. Therefore, identifying the rockfall potential source areas by using Eq. 1 should be evaluated by the user considering the reality of the in situ condition. In other words, Eq. 1 can only be interpreted as a simple empirical relationship which leads the user to possible potential source areas having steep topography

depending on the resolution of DEM rather than the whole study area. Due to the nature of the empirical process, it is open to user intervention by considering the reality of the study area.

The jointed granodiorite rock mass extends over a big area as a wide arc shaped from the northwest to the southeast in the north-east of the district. By considering the value of the general aspect of rock slope surfaces, the dip direction and the dip aperture range were used as  $210^\circ$  and  $60^\circ$ , respectively, in Conefall v1.0 program. After identifying the rockfall potential source areas, the propagation zones and the percentage of the fallen rock blocks within the propagation zones for the Sivrihisar residential area were determined by following the same procedure with the procedure considered for the Kargabedir Hill rockfall area (Fig. 10 and Table 2).

#### Proposal of an innovative methodology for the adjustable use of energy line angle for rockfall susceptibility mapping

The outer border of the rockfall susceptibility mapping, which aims to determine the farthest stopping points that the fallen rock blocks can reach, should cover theoretically 100% of the fallen or possible fallen rock blocks from the rockfall source area. Therefore, it is of utmost importance to select the value of  $ELA_{\max\_stop}$  that aligns



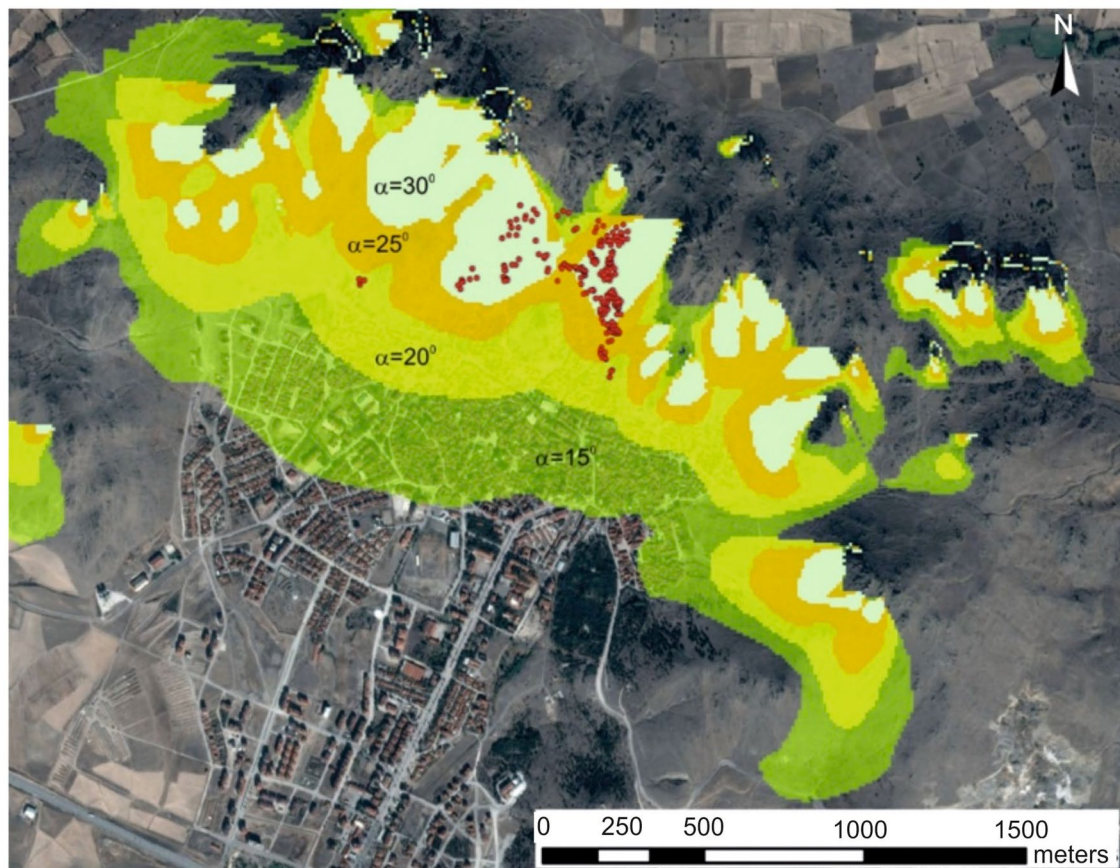


**Fig. 10** Propagation zones for different energy line angle values in the Sivrihisar residential rockfall region (from Kalender 2017)

with the characteristics of the study area in order to prepare a realistic rockfall susceptibility map. As mentioned before, the three main input parameters such as the rockfall source area, DEM, and energy line angle are taken into consideration for mapping of the rockfall propagation zone.

A statistical evaluation of the energy line angle values to be considered for the maximum run-out distance compiled from the literature has been done by Larcher et al. (2012) (Table 3). As it is seen in Table 3, the lowest, average, and highest values are 26.57°, 31.14°, and 36.87°, respectively. In addition, Larcher et al. (2012) also performed a statistical analysis of the database of the Northern Alps in France (Table 4). The researchers proposed a classification to define

the rockfall susceptibility (intensity of exposure to rockfall events) considering the possible percentages of rock blocks in the maximum run-out zone represented by the different energy line angles of the data from the Northern Alps in France (Table 5). Although the values of susceptibility threshold slope angle in the classification presented in Table 5 may be applicable for the Northern Alps in France, it is obvious that the ELA angle values will be expected to be different for the different areas. Therefore, the application of this classification with its current form to the different sites has

**Table 2** The percentage of the rock blocks within the propagation zones for the Sivrihisar rockfall area (from Kalender 2017)

Energy line angle (°)	Rock block percentage (%)
15	100
20	95.3
25	76.4
30	33.3

**Table 3** Statistical distribution of minimal and maximal energy line angle values (Larcher et al. 2012)

Statistics	Minimal energy line angle (°)	Maximal energy line angle (°)
Mean	31.14	39.30
Minimum	26.57	30
1st quartile	29.45	36.97
2nd quartile	31.61	38.58
3rd quartile	33	41.80
Maximum	36.87	48.99

**Table 4** The ELA values corresponding to rock block percentages in the French Northern Alps rockfall database (Larcher et al. 2012)

Energy line angle (ELA) (°)	Rock block percentages (%)
24.65	0.001
28.0	4.0
30.0	9.0
32.0	20.0
34.0	35.0
35.0	40.0
38.0	65.0

the potential to produce unrealistic results in terms of degree of susceptibility to rockfall.

The data belong to some researchers in the literature regarding the percentage of blocks stopped in the area above the energy line angle is given in Fig. 2. As seen in Fig. 2, it has been defined as an S-shaped curve relationship that provides the best possible distribution by ignoring data belonging to Toppe (1987). This S-shaped curve seems compatible with the cumulative normal distribution relationship. Accordingly, the number of the rock blocks is less for high ELA values in close vicinity of the rockfall source area; vice versa, it increases for low ELA values away from the rockfall source area. Based on the limited literature cases, it was plotted between energy line angles equal to 24° and 33° for 100% of the fallen rock blocks stopped above the energy line angle (see Fig. 2). The main reason for the range about 10° may be related with the differences in the maximum run-out distance depending on the characteristics of the studied rockfall area itself. From a general point of view, the site-dependent characteristics can be divided into two groups: while the first one is related to the rock blocks such as shape and angularity, the second one is about the surface properties of the slope where the rock blocks propagate.

A new term called as  $ELA_{max\_stop}$  was defined to represent the energy line angle that extends to the border of the propagation zone as the maximum run-out distance that is obtained from application of the cone approach to all points (pixels) in source area. The slope angle denoted as  $\alpha$  is a threshold angle of the steep

**Table 5** The geometrical ELA thresholds for rockfall run-out zone classification (modified from Larcher et al. 2012)

Geometrical ELA thresholds (°)	Probability of rockfall propagation	Rock block percentages (%) in the run-out zone
$\geq 38$	High	65 and higher
$35 \geq 38$	Medium	40–65
$32 \geq 35$	Low	20–40
$28 \geq 32$	Very low but not null	4–20

areas to be used for identifying potential rockfall source areas by using DEM. Conceptually, all fallen rock blocks in a rockfall-prone area stop within the cone propagation zone. The cone propagation zone is bounded by the border of the source area produced by using the threshold angle ( $\alpha$ ) on DEM and the maximum run-out border of the propagation zone obtained from the application of cone approach to all points in the source area by using  $ELA_{max\_stop}$ . In other words,  $\alpha$  and  $ELA_{max\_stop}$  are two important energy line angle values to be considered as two extreme values in the cone propagation approach. Therefore, the use of a unique S-shaped distribution, which is defined by a single curved line defined in Fig. 2 for different areas, is not possible and realistic due to the specific site-dependent conditions of each rockfall-prone area. In fact, the S-shaped curve distribution between  $\alpha$  and  $ELA_{max\_stop}$  as the extreme values seems more realistic and meaningful for the purpose of producing the rockfall susceptibility map.

In the susceptibility classification based on the adjustable  $ELA_{max\_stop}$ , some arrangements for the specific conditions of different areas have been made in accordance with the S-shaped distribution curve. In the susceptibility classification, while the “High susceptibility” class starts from the border of the source areas which means almost all the fallen rocks block pass, the “Very Low susceptibility” class ends with the energy line angle targeting the maximum run-out distance. Fewer rock blocks stop-over in the high susceptibility class area, while almost any falling blocks pass through this area once. On the other hand, the very low susceptibility class is further away from the source area, and the rock blocks in other susceptibility classes beyond this zone, as a result of depletion of their energy, cannot reach this area. Due to the proposed classification being a spatial evaluation, it may be defined as the intensity of exposure from the rockfall events which may be defined as the rockfall susceptibility. The threshold ELA values of the five susceptibility classes will be different for every case based on the values of  $\alpha$  and  $ELA_{max\_stop}$ . Therefore, the new proposed classification procedure needs an adjustable S-shaped curve which starts from threshold slope value ( $\alpha$ ) for the potential source areas of the studied area based on the resolution of DEM and ends with  $ELA_{max\_stop}$ . In addition to the cases belonging to Onofri and Candian (1979) and Larcher et al. (2012), two cases were studied, namely Kargabedir Hill and Sivrihisar residential rockfall areas, presented by more than 1 point on the graph of the value of ELA versus the percentage of rock blocks stopped above the energy line angle. Of course, the different S-shaped curves were drawn for each of four cases (Fig. 11a). However, the best fitting curve presentation of four cases by a single S-shaped curve is not possible because each case has different values of  $\alpha$  and  $ELA_{max\_stop}$  (Fig. 11a). In other words, the values of the extreme energy line angles of the sensitivity classes are different from each other due to the different values of  $\alpha$  and  $ELA_{max\_stop}$  for each case. As discussed before, the S-shaped curves start from the threshold slope angle value ( $\alpha$ ) for definition of the potential source areas. Another parameter of the curve that separates the rockfall susceptibility classes is the energy line angle ( $ELA_{max\_stop}$ ) targeting the furthest stopping border of the propagation zone. As seen in Fig. 11a, the data points of Onofri and Candian (1979) were placed on the steepest S-shaped curve. By considering this fact, firstly data points of each case grouped on their own S-shaped curve were shifted to fix on a point of the





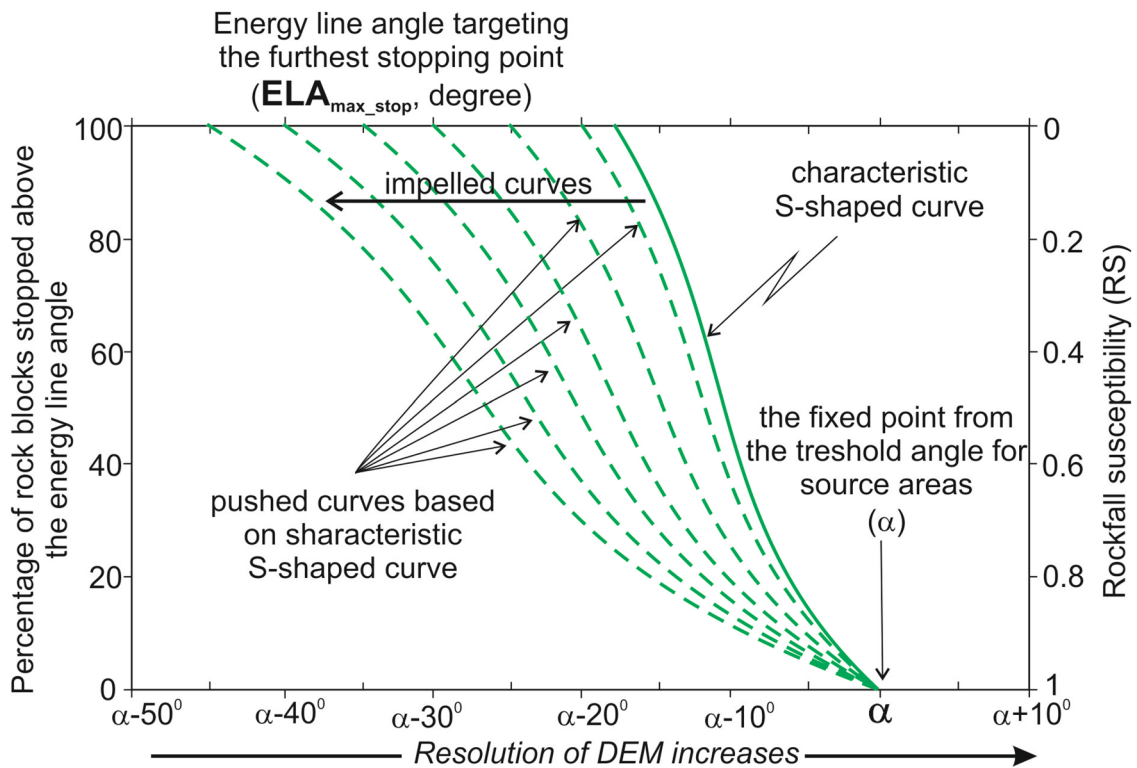


**Fig. 12** The generalized S-shaped distribution curves obtained from the characterized S-shaped curve by considering the possible values of  $ELA_{max\_stop}$  and  $\alpha$

is given in Fig. 13, the interpolation technique can be applied for selection of the curve using determination of boundary ELA values for each susceptibility class. In addition to these graphical presentations of the S-shaped curves, which can be used for interpolation to obtain a curve to be considered for the studies case, a series of equations were also generated at the end of this study for the general practical use of the proposed classification.

#### An initial attempt to a rating-based classification for preliminary selection of the $ELA_{max\_stop}$

The use of energy line angle for rockfall mapping is highly practical; however, the selection of  $ELA_{max\_stop}$  which varies in quite wide ranges within about from 15 to 50°, may be evaluated as the most critical stage. Even a preliminary guide has not been presented in the literature for selection of  $ELA_{max\_stop}$ . Of course, the practitioner can prefer the use of 15° from the conservatively point of view; however, to be too conservative may not be economical in engineering perspective. In this study, a rating-based attempt, namely RDR, was made for only a connection between 15 and 45° which was used instead of 50° to be on the safe side.

For this purpose, an initial proposal for a RDR system was introduced for the preliminary determination of  $ELA_{max\_stop}$ . The suggested supportive approach to the practitioners for determination of  $ELA_{max\_stop}$  which targets the possible furthest stopping border for the fallen rock blocks, should be considered as an initial attempt with its flexibility to open improvement. By using the proposed approach, the value of

$ELA_{max\_stop}$  should not be perceived as an indispensable value; however, it can be considered as a preliminary default value open to user control. Therefore, it should be emphasized that the initial form of the RDR system is open to improvement, as in other empirical approaches in literature, with additions of new parameters and new data. The supportive approach for determining  $ELA_{max\_stop}$  should be regarded as a starting point in the literature and should remain open for further refinement by considering new parameters and new cases.

Ritchie (1963) stated that the maximum run-out distance of the fallen rock block is controlled by the rockfall source area (starting point), block shape and geometry, surface topography, and mechanical properties of the rock mass. The run-out distance of a fallen rock block is mainly influenced by both parameters related with the rock blocks and characteristics of slope surface. In this study, to relatively simplify the structure of the RDR system, the prominent parameters on the maximum run-out distance of rockfall events were taken into consideration. However, the preferred parameters in this study should not be interpreted as there are no other parameters that may be effective on run-out distance, because it should be taken into consideration that RDR system is open to improvement.

The following parameters were preferred in the structure of RDR system.

- (i) Parameters related to rock blocks
  - (a) Shape of rock blocks

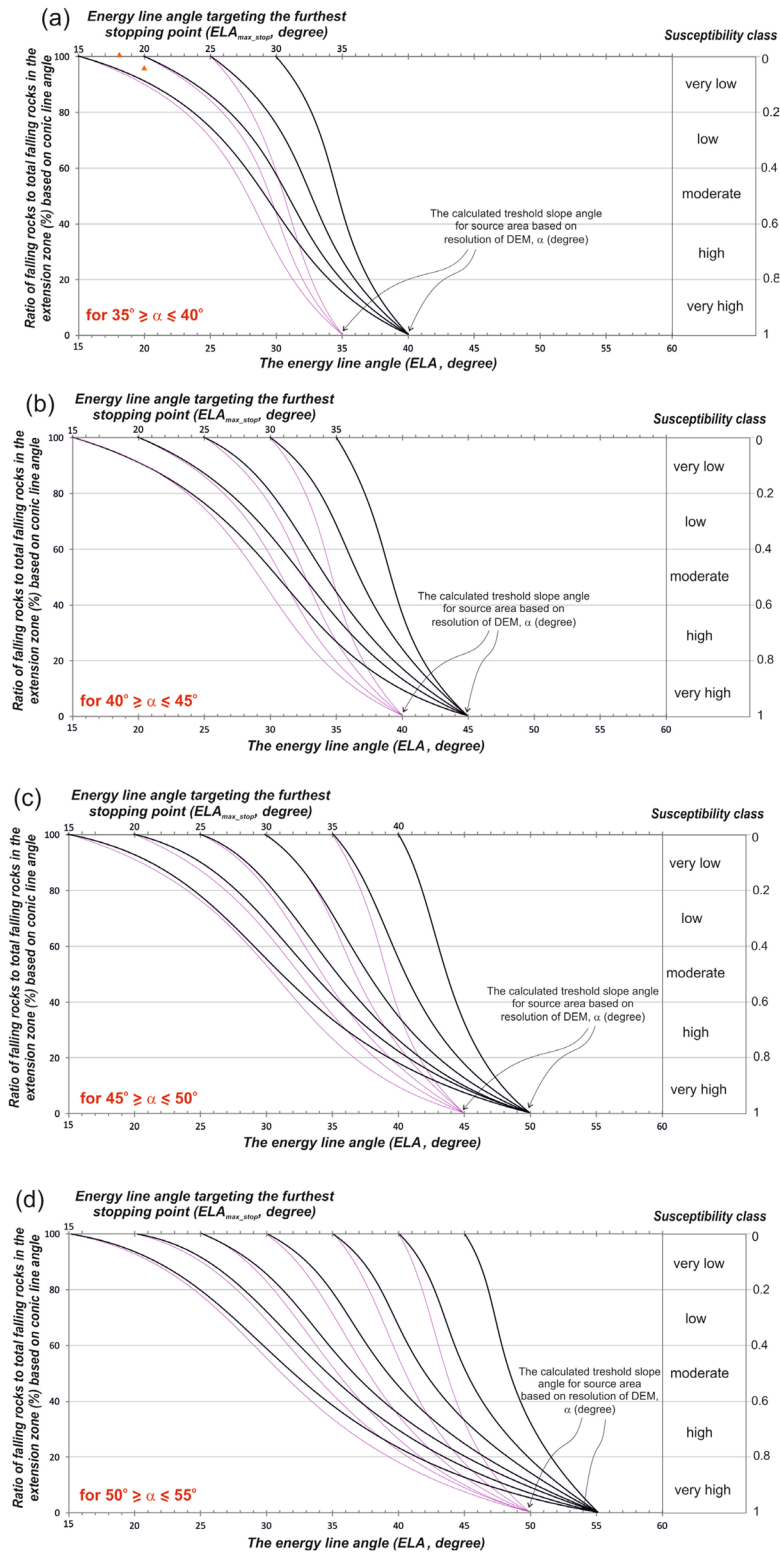


**Fig. 13** Curvilinear distribution relations plotted for potential  $ELA_{max\_stop}$  values. Source area threshold angles ( $\alpha$ ) are **a**  $35^\circ$  and  $40^\circ$ , **b**  $40^\circ$  and  $45^\circ$ , **c**  $45^\circ$  and  $50^\circ$ , and **d**  $50^\circ$  and  $55^\circ$  (from Kalender 2017)



- (b) Angularity of rock blocks
- (ii) Parameters related to slope surface
  - (a) Slope surface characteristics (normal and tangential coefficient of restitution)
  - (b) Slope surface roughness (friction resistance of slope surface,  $\phi$ )

The most difficult stage of developing a rating-based empirical approach is the apportionment of total rating to the input parameters. As an initial attempt, the contributions of the related two parameters on the run-out distance of a fallen rock block were assumed as equal. Therefore, the maximum rating of RDR equal to 100 was divided by 2 for the parameters related to rock blocks and the parameters related to slope surface.

**Shape of rock blocks** As expected usually, the “equidimensional” shaped rock blocks reach longer run-out distances, when compared with the “flat/plate” shaped rock blocks that have one dimension less than the others. The flat/plate-shaped rock block generally slides on its large surface rather downward than rolling around itself. Therefore, the maximum run-out distance of the flat/plate-shaped rock blocks is generally expected as less when compared with the movement of “equidimensional block” shaped rock blocks which have better bouncing and rolling ability on slope surface. On the other hand, when “columnar” shaped rock blocks are evaluated in terms of run-out distance, it may be described between the equidimensional and the flat/plate-shaped rock blocks. Depending on the three dimensions of a rock block, the transition among these three main block shapes to each other may be usual in nature. To meet three main rock block shapes with possible transition among them, a triangular rating chart was preferred (Table 6 (a)).

**Angularity of rock blocks** Another rock block property that has an effect on the run-out distance is the angularity of the rock blocks. As a physical expectation, on the same slope surface when the angularity of the equidimensional shaped rock blocks decreases, it is usual for a fallen rock block to reach further distances. This situation is closely related to the friction between the fallen rock block and slope surface. In other words, the run-out distance of the rounded blocks will be longer than that of angular blocks on the same slope surface. By considering the effect of angularity of the fallen rock blocks on run-out distance, a rating based on angularity description of rock blocks from the angular to the rounded was introduced to the rating system (Table 6 (b)).

**Slope surface characteristics** During the bouncing motion of a falling rock block, some amount of the kinetic energy (or its normal and tangential velocities) is absorbed by every impact between slope surface and rock block. The velocity and energy of a fallen rock block gradually decrease within the run-out distance. Therefore, the cover material of the slope surface plays an important role in the degree of kinetic energy restitution to a fallen rock block. The normal and tangential coefficients of restitution vary depending on the cover material of slope surface such as vegetation, talus, or bare rock. The site-specific normal and tangential coefficients of restitution can be determined by back analyses of the fallen rock blocks. Since the back analyses are not always possible, the numerous normal and tangential coefficients of restitution values are also available in the literature presented by various researchers based

on different slope surface conditions (Crosta and Agliardi 2003; Dorren 2012; Rocscience Inc. 2017).

In order to select the slope surface characteristic rating, a chart was developed by using the normal and tangential coefficients of restitution ( $R_n$  and  $R_t$ ). Data pairs of  $R_n$  and  $R_t$  are listed by Rocscience Inc. (2017). In the developed chart, the rating ranges equally partitioned by 5-point intervals (Table 6 (c)).

**Slope surface roughness (friction resistance of slope surface,  $\phi$ )** Another selected parameter which can be considered as a complement to the slope surface characteristic rating is slope surface roughness (friction resistance of slope surface,  $\phi$ ). The friction resistance between the rock block and the surface is significantly affected by the roughness of the surface as well as the shape and angularity of the rock block. The friction resistance between the fallen rock block and the slope surface is significantly affected by the roughness of the surface as well as the shape and angularity of the rock block. While the frictional resistance of the rough slope surface is high, the expected run-out distance decreases. On contrary, with the smooth slope surface having low friction resistance, the falling rock block can move towards further far the stop point. The friction resistance which can be defined by the friction angle ( $\phi$ ) of the surface can be obtained from Eq. 2 by using the tangential coefficient of restitution ( $R_t$ ) (Rocscience Inc. 2017). It should be noted that this equation is empirical and produces very high  $\phi$  values, especially when  $R_t < 0.55$ . By considering the value of  $\phi$  obtained from Eq. 2, a rating was introduced to the RDR system (Table 6 (d)). In addition to the  $R_t$  values listed by Rocscience Inc. (2017), numerous alternative recommendations are also available in literature for selection of the value of  $R_t$  based on description of slope surface.

$$\phi(\text{radians}) = \left( \frac{1 - R_t}{R_t} \right) \text{ or } \phi(\text{degrees}) = \frac{180}{\pi} \left( \frac{1 - R_t}{R_t} \right) \quad (2)$$

When the slope surface is not composed of or covered by a single material, it may be questioned how the single values for each of tangential and normal coefficients of restitution ( $R_t$  and  $R_n$ ) can be selected. Considering that the empirical approaches are user-controlled methods oriented to the solution of a problem, depending on the importance of the case, either conservative  $R_t$  and  $R_n$  values or the weighted average values of  $R_t$  and  $R_n$  for different cover material in the field may be selected.

Increasing or decreasing effects on the run-out distance of four selected parameters used in the RDR system were discussed above by taking into account some physical rules and expectations. Although the maximum 100 rating of RDR is divided equally between two sub-groups as the parameters related to rock block and slope surface, slightly different weights were considered for each parameter under two sub-groups. For two sub-parameters related to rock blocks, while the degree of angularity of a fallen rock block generally affects the run-out distance by rolling and sliding motion, the shape of rock block also plays a role on the bouncing motion in addition to rolling and sliding motion of a fallen rock block. Therefore, heuristically, while the maximum rating contribution of rock block shape was taken as 30, the remaining 20 points was used for maximum rating of angularity of rock block (Table 6). Similarly for two sub-parameters related to slope surface, while slope surface characteristic was defined by using both normal and

**Table 6** The proposed maximum run-out distance rating (RDR) classification (from Kalender 2017).

(a) Rating for shape of rock blocks ( $R_{BS}$ )			
Description →	Equidimensional	Columnar	Flat/plate
Rating ( $R_{BS}$ ) →	0	20	30

(b) Rating for angularity of rock blocks ( $R_{BA}$ )				
Description →	Angular	Sub-angular	Sub-rounded	Rounded
Rating ( $R_{BA}$ ) →	20	12.5	5	0

(c) Rating for slope surface characteristics (normal and tangential coefficient of restitutions) ( $R_{SC}$ )	
Description → Rating ( $R_{SC}$ ) →	

Description → Rating ( $R_{SC}$ ) →	
--	--

\*: Prediction of  $R_T$  and  $R_n$  coefficient numbers according to surface properties can be made from Roescience Coefficient of Restitution Table

(d) Rating for friction resistance of slope surface ( $\phi$ ) (from Eq.2) ( $R_\phi$ )					
Description →	$\phi \geq 40^\circ$	$\phi = 30^\circ$	$\phi = 20^\circ$	$\phi = 10^\circ$	$\phi \leq 5^\circ$
	very high	high	moderate	low	very low
Rating ( $R_\phi$ ) →	20	15	9	3	0

Rating relation based on the value of  $\phi \rightarrow R_\phi = 0.6\phi - 3$

tangential coefficients of restitutions, friction resistance of slope surface was defined by  $\phi$  based on only tangential coefficient restitution. By considering complementary feature of friction resistance to slope surface characteristic, heuristically, while the maximum rating contribution of slope surface characteristic was taken as 30, the remaining 20 points was used for maximum rating of friction resistance of slope surface (Table 6).

The value of RDR and run-out distance are inversely related; as the value of RDR increases, the run-out distance of fallen rock blocks decreases. In other words, the rock blocks are equidimensional and “rounded,” and where a high coefficient of restitution is observed along bare hard rock profiles, the value of RDR decreases towards zero, indicating longer run-out distances (Table 6). However, it should be underlined that the maximum

rating weight of the four sub-parameters is open to improvement by new case studies similarly to other rock engineering rating systems such as RMR. While the value of RDR varies between zero and 100, the higher RDRs mean shorter run-out distance of the fallen rock blocks. Besides, there is an inverse relation between  $ELA_{max\_stop}$  and run-out distance due the geometrical relation between two of them. In this study, the starting and ending RDR and  $ELA_{max\_stop}$  pairs as the boundary condition were defined based on literature findings. However, the relation between RDR and  $ELA_{max\_stop}$  was tried to improve by considering three cases. For this purpose, an additional case which was studied by Aksoy and Ercanoglu (2006) was also taken into consideration in addition to two cases from Kargabedir Hill and Sivrihisar residential area. The rockfall area of Ankara andesite bare rock outcrops, where Ankara Castle is also located, was studied by Aksoy and Ercanoglu (2006). Ankara andesite rock mass outcrops observed around Ankara Castle include six joint sets, and mean spacing of discontinuity sets varies from 0.21 to 0.39 m (Fig. 14a). Therefore, the shape of the rock blocks can be assumed as equidimensional

(Fig. 14b, c). The ELA values of the fallen rock blocks by using a line from the source point to the stop point were calculated by Prof. Dr. M. Ercanoglu for this study. The graphical presentation of the calculated ELA values of the fallen blocks and  $ELA_{max\_stop}$  are given in Fig. 14d. While  $ELA_{max\_stop}$  was obtained as  $21^\circ$ , the tangential and normal coefficients of restitution  $R_t$  and  $R_n$  for the case studied by Aksoy and Ercanoglu (2006) were selected as 0.910 and 0.487 by considering bare rock slope according to a list given by Rocscience Inc. (2023), respectively.

In addition to the energy line angle, values for the maximum run-out distances ( $ELA_{max\_stop}$ ) obtained from the studies of various researchers in the literature and the values of Sivrihisar residential, Kargabedir Hill, and Ankara Castle rockfall areas investigated in this study are shown in Fig. 15. As mentioned before, in the cone propagation approach, the maximum run-out distances of border propagation zone are drawn by using the energy line angle named as  $ELA_{max\_stop}$ . By considering the possible values of the energy line angle values for the maximum run-out distance given in Fig. 15, the possible highest and lowest  $ELA_{max\_stop}$  values were accepted as  $15^\circ$

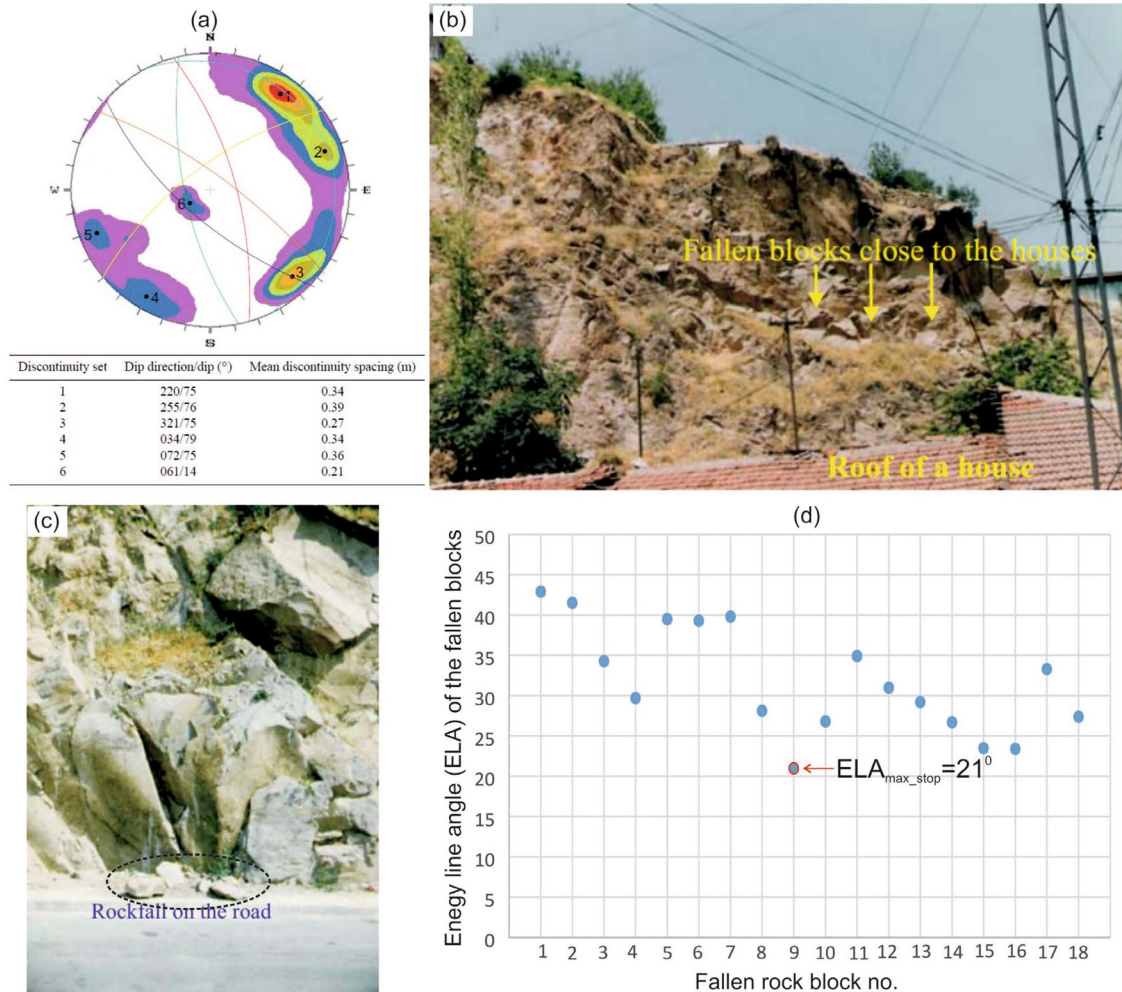


**Fig. 14** a Presentation of the main discontinuity sets and characteristics of the discontinuities. b, c Ankara andesite rock mass outcrops observed around Ankara Castle and the views of Ankara andesite outcrops (from Aksoy and Ercanoglu 2006). d The graphical presentation of the calculated ELA values of the fallen blocks and  $ELA_{max\_stop}$  (calculated by Prof. Dr. M. Ercanoglu)

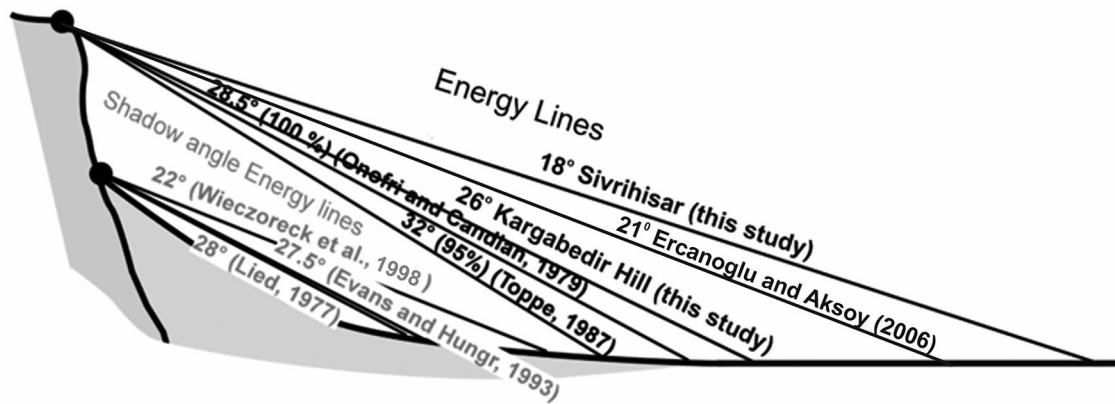


**Fig. 15** Energy line used for the cone method from the top or the bottom of a cliff (shadow angle), according to various authors and the rockfall sites investigated in this study (modified by from Jaboyedoff and Labiouse (2003) after Crosta et al. (2001))

and  $45^\circ$  for the values of RDR equal to 0 and 100, respectively. Of course, the relation between two starting and ending data pair needs to be clarified. It is possible to use a simple linear relation between RDR and  $ELA_{\max\_stop}$  by considering two RDR and  $ELA_{\max\_stop}$  pairs as the starting and the ending points (Fig. 16a).

However, the relation from the lowest to highest  $ELA_{\max\_stop}$  depending on RDR may not be related not only to the value of RDR but also to the morphology of slope surface such as convex or concave in horizontal and/or profile plane. This and similar other innovative issues can be considered as a new research topic for furure studies. In this study, it was preferred that even a slightly improvement can be investigated on the relation between RDR and  $ELA_{\max\_stop}$  by using three cases as follows.

While RDR for the Ankara Castle rockfall area was determined as 33.6, RDR was determined as 46 and 26 for Sivrihisar residential and Kargabedir Hill and rockfall areas, respectively (Table 7). On the other hand, the values of  $ELA_{\max\_stop}$  obtained from the field measurements were  $26^\circ$ ,  $18^\circ$ , and  $21^\circ$  for Kargabedir Hill, Sivrihisar residential area, and Ankara Castle rockfall area, respectively. Three RDR and  $ELA_{\max\_stop}$  pairs were plotted on the graph together with two RDR and  $ELA_{\max\_stop}$  pairs for the lowest and highest  $ELA_{\max\_stop}$  values. As seen in Fig. 16a, slightly downward curvilinear relation (Eq. 3a), which seems more representative for the plotted data, was investigated by trial-and-error method. The relation between RDR and a constant ( $\Delta$ ), which may be taken into consideration to stay on the safe side, was also investigated by using 10% of the measured  $ELA_{\max\_stop}$  values (Eq. 3b and Fig. 16b). In this stage, it needs to be noticed that the values of  $\Delta$  equal to 0 and 4.5 were used for RDR = 0 and RDR = 100, respectively.

$$ELA'_{\max\_stop} = \frac{RDR}{(120 - RDR)^{0.4}} + 15 \quad (3a)$$

$$\Delta = 0.2761(RDR)^{0.6} \quad (3b)$$

$$ELA_{\max\_stop} = ELA'_{\max\_stop} - \Delta \quad (3c)$$

and Ankara Castle rockfall areas were used as inputremind again, the determined value of  $ELA_{\max\_stop}$  by using the proposed approach in this study is not an indispensable value; however, it can be taken into consideration as a preliminary default value open to user control.

The values of RDR for Kargabedir Hill, Sivrihisar residential, and Ankara Castle rockfall areas were used as input in Eqs. 3a to 3c, and the values of  $ELA_{\max\_stop}$  were obtained as  $20.5^\circ$ ,  $17.2^\circ$ , and  $18.6^\circ$ , respectively. The values of  $ELA_{\max\_stop}$  determined from Eqs. 3a to 3c were slightly less than field study-measured values due to the use of  $\Delta$  as a safety reduction parameter. It can be stated that the calculated values of  $ELA_{\max\_stop}$  were acceptable for rockfall susceptibility mapping when compared with the measured values in the field studies.

#### Application of the innovative methodology to the Kargabedir Hill and Sivrihisar residential rockfall areas

As in detail given above, an innovative methodology for the adjustable use of energy line angle for susceptibility mapping was introduced to the cone propagation approach. The implementation steps of the innovative proposal are as follows:

- Step 1: The possible source areas are mapped by using threshold slope angle ( $\alpha$ ) obtained from Eq. 1. Of course, it is possible to re-evaluate the possible rockfall source areas obtained from the empirical relation.
- Step 2: The value of RDR for the studied case is determined by using the ratings of the parameters used in the RDR system.
- Step 3: The energy line angle ( $ELA_{\max\_stop}$ ) is determined from Eqs. 3a to 3c by using the value of RDR. The value of  $ELA_{\max\_stop}$  obtained from Eqs. 3a to 3c can be taken into consideration as a preliminary default value open to user control.
- Step 4: According to threshold angles ( $\alpha$  and  $ELA_{\max\_stop}$ ), the suitable graphic is selected from Fig. 13. By considering the  $ELA_{\max\_stop}$  value, the suitable S-shaped curve for the case on the selected graph is used. Hence, if it is necessary, interpolation can be made for selection of suitable curve.



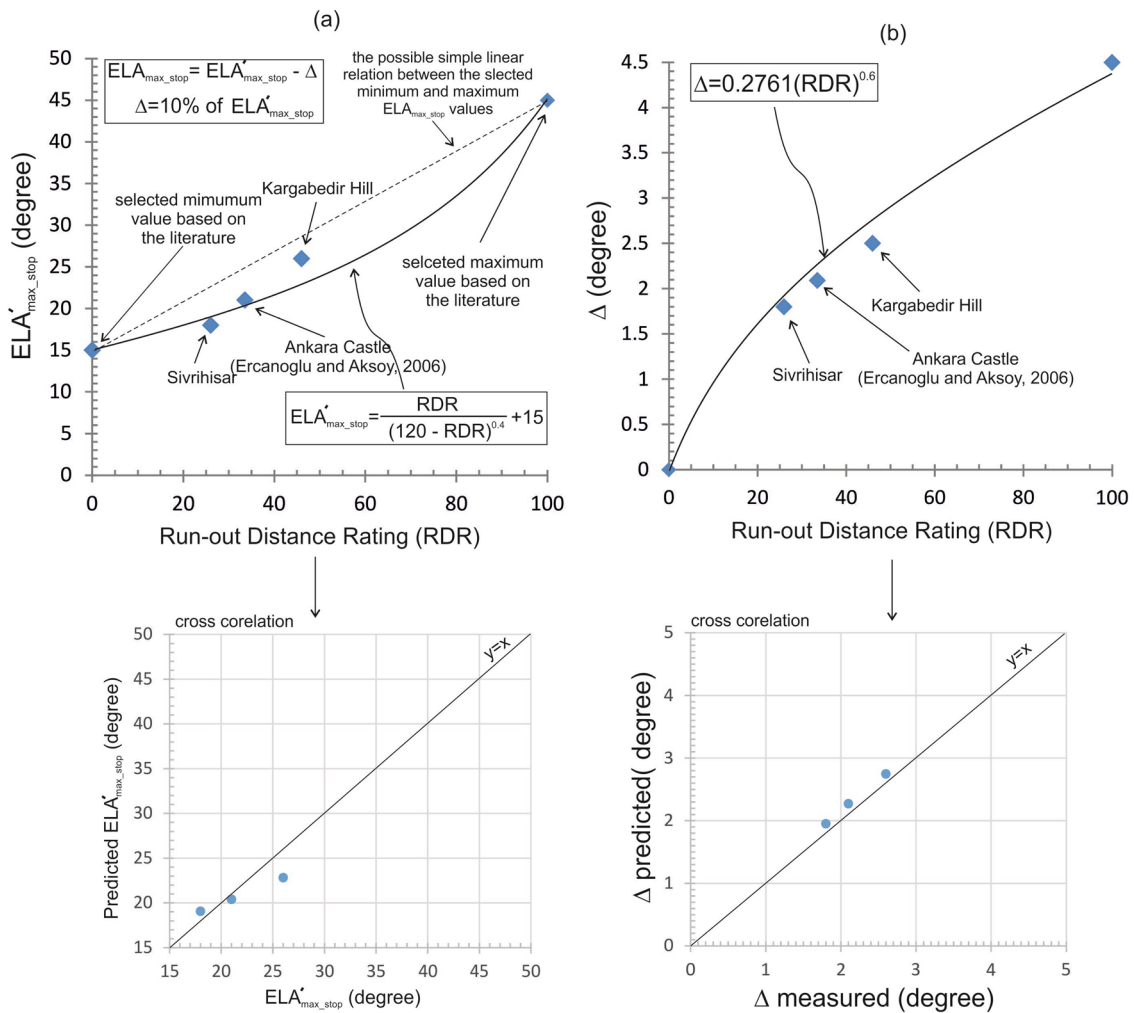


**Fig. 16** The proposed relations between the RDS and  $ELA'_{max\_stop}$ . **a** Root of the equation ( $ELA'_{max\_stop}$ ) and **b** the reduction value ( $\Delta$ ) for being on the safe side based on uncertainties (modified from Kalender 2017)

- Step 6: On the S-shaped curve, the ELA values for the boundary values of the rockfall susceptibility classes on the right side of the graph are determined. Practically, Eqs. 4a to 4f (given under section “Development of practical equations for the determination of the values of ELA for the rockfall susceptibility classes”) derived based on  $\alpha$  and  $ELA'_{max\_stop}$  and presented under the subsequent title can be used for the same purpose instead of the use of graphical presentations.
- Step 7: Cone propagation zones and, if desired, velocity and kinetic energy values can be produced by using Conefall v1.0 software, considering the energy line angle value determined for each sensitivity class.
- Step 8: Finally, a suitable GIS program is used to convert Conefall v1.0 output files to maps.

The implementation steps of the innovative methodology were carried out in the Kargabedir Hill and Sivrihisar residential rockfall areas.

#### Kargabedir Hill rockfall area

In the first stage of the rockfall mapping, the rockfall potential source area in the Kargabedir Hill rockfall area was identified by using the value of  $\alpha = 52^\circ$  determined for  $RES = 2$  m from Eq. 1. As suggested in step 3 given in the previous section, among the plotted curvilinear distribution relations given in Fig. 13, the one having a source area threshold angle between  $50$  and  $55^\circ$  (Fig. 13d) was selected. In addition, the  $ELA'_{max\_stop}$  value was determined as  $20.5^\circ$  for the  $RDR = 46$  (Table 7). The boundary values of ELA for five susceptibility classes were determined for the Kargabedir Hill rockfall area by using the interpolated curve drawn for two threshold values such as  $\alpha = 52^\circ$  and  $ELA'_{max\_stop} = 20.5^\circ$  (Fig. 17, Table 8). Boundaries of rockfall propagation zone of the Kargabedir Hill rockfall area within five susceptibility zones were analyzed by Conefall v1.0 program for each ELA value by using the “asci” file of the high-resolution DEM, the asci file of the source



**Table 7** Evaluation of the Kargabedir Hill and Sivrihisar residential rockfall areas in RDR classification (from Kalender 2017)

Input parameter of RDR		Kargabedir Hill		Sivrihisar residential area		Ankara Castle area	
	Description	RDR	Description	RDR	Description	RDR	Description
$R_{BS}$	1 dimension is slightly longer than the other 2, so it is on the equidimensional-columnar-shaped edge of the identification triangle but closer to the equidimensional-shaped	5	Equidimensional-columnar and partly plate-shaped but closer to the definition of equidimensional	7	The rock blocks are almost equidimensional	5	
$R_{BA}$	Sub-angular blocks	12.5	Sub-rounded and sub-angular blocks	7	Angular blocks	20	
$R_{SC}$	Semi-buried and fallen large block on the talus deposit Coefficient of restitution table given by Rocscience <sup>a</sup> $R_n = \sim 0.3$ and $R_t = \sim 0.65$	13	Talus cover with vegetation Coefficient of restitution table given by Rocscience <sup>a</sup> $R_n = \sim 0.33$ and $R_t = \sim 0.83$	8	Bare rock slope Coefficient of restitution table given by Rocscience <sup>a</sup> $R_n = \sim 0.487$ and $R_t = \sim 0.910$	7	
$R_\phi$	Slope surface is smooth, but there are large fallen and semi-buried blocks on $\phi = 30.9^\circ$ (calculated from Eq. 2)	15.5	Slope surface is smooth, but there are large fallen blocks on $\phi = 11.7^\circ$ (calculated from Eq. 2)	4	Slope surface clean $\phi = 7.7^\circ$ (calculated from Eq. 2)	1.6	
Total RDR		46	26	33.6			
$ELA_{max\_stop}$ measured by the field studies		26	18°	21°			
$ELA_{max\_stop}$ obtained from Eqs. 3a to 3c		$\sim 20.5^\circ$ ( $ELA'_{max\_stop} = 23.2^\circ$ and $\Delta = 2.7^\circ$ )	$\sim 17.2^\circ$ ( $ELA'_{max\_stop} = 19.2^\circ$ and $\Delta = 2^\circ$ )	$\sim 18.6^\circ$ ( $ELA'_{max\_stop} = 20.6^\circ$ and $\Delta = 2.3^\circ$ )			

<sup>a</sup>Web address of Rocscience coefficient of restitution table in RocFall in February 2023 is <https://www.roccscience.com/help/rockfall/documentation/slope/materials/reference-tables/roccscience-coefficient-of-restitution-table-in-rockfall>

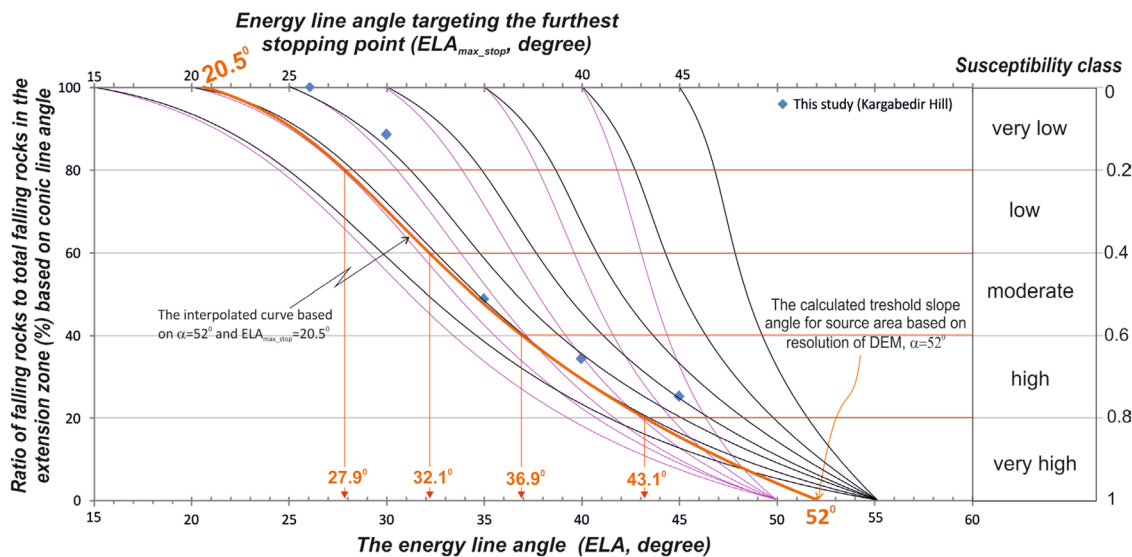


**Fig. 17** Determination of the susceptibility boundary ELA values for the Kargabedir Hill rockfall area obtained from the interpolated curve on curvilinear distribution relations for the source area threshold angles 50° and 55° (from Kalender 2017)

areas, and the ELA values which are listed in Table 8 (see also Fig. 18). By overlapping the propagation zones determined for these five limit values, rockfall susceptibility map of Kargabedir Hill was produced (Fig. 19).

#### Sivrihisar residential rockfall area

The 10 × 10 m resolution DEM of the Sivrihisar residential rockfall area was obtained from the 1/25,000-scale topographic map. Of course, the use of low-resolution DEM has negative effects on mapping for small rockfall susceptible areas, especially when the innovative new methodology is not taken into consideration. However, to overcome this negative limitation, the new methodology was applied by considering the innovative improvements about the use of low-resolution DEMs. As given in detail previously, the threshold slope angle of source areas was determined as  $\alpha = 35^\circ$  and the  $ELA_{max\_stop}$  value was calculated as  $17.2^\circ$  for the Sivrihisar residential rockfall area. The boundary ELA values for five susceptibility classes were determined on graphical presentation as shown in Fig. 20. The boundary values of ELA were presented together with the susceptibility values in Table 9. For the susceptibility classes given in Table 9, intensity of exposure to rockfall susceptibility map for the Sivrihisar residential rockfall area was produced by following the procedure applied to the Kargabedir Hill rockfall area (Fig. 21).

#### Development of practical equations for the determination of the values of ELA for the rockfall susceptibility classes

For the use in the cone propagation approach, an innovative methodology has been developed for the determination of the boundary values of ELA among different sensitivity classes in the rockfall susceptible area within the threshold slope angle of the source areas ( $\alpha$ ) and  $ELA_{max\_stop}$ . As in detail discussed above, a series of graphical presentations to be used by the interpolation technique

for defining a representative S-shaped curve based on the values of  $\alpha$  and  $ELA_{max\_stop}$  are presented in Fig. 13. However, the use of interpolation technique on the S-shaped graphical presentations given in Fig. 13 requires a drawing process by practitioner control. In this stage of the study, a series of equations were developed to define the S-shaped curve to be obtained by the interpolation technique on the curves given in Fig. 13 by using the inputs of  $\alpha$  and  $ELA_{max\_stop}$ . The required S-shaped equation, which considers  $\alpha$  and  $ELA_{max\_stop}$  as inputs, was investigated by trial-and-error technique on the general form of the S-shaped function given in Eq. 3d.

$$S(x) = \left( \frac{1}{1 + e^{-kx}} \right)^a \quad (3d)$$

While determination of rockfall susceptibility (RS) for any ELA value based on  $\alpha$  and  $ELA_{max\_stop}$  can be calculated by using Eqs. 4a–4f, the determination of ELA value for any rockfall susceptibility value based on  $\alpha$  and  $ELA_{max\_stop}$  is also possible by using Eqs. 4a–4f.

**Table 8** ELA ranges for susceptibility classes of the Kargabedir Hill rockfall area (from Kalender 2017)

Susceptibility classes	Susceptibility values	ELA ranges for each susceptibility class (°)
None	0	< 20.5
Very low	0.2	20.5–27.9
Low	0.4	27.9–32.1
Medium	0.6	32.1–36.9
High	0.8	36.9–43.1
Very high	1	> 43.1

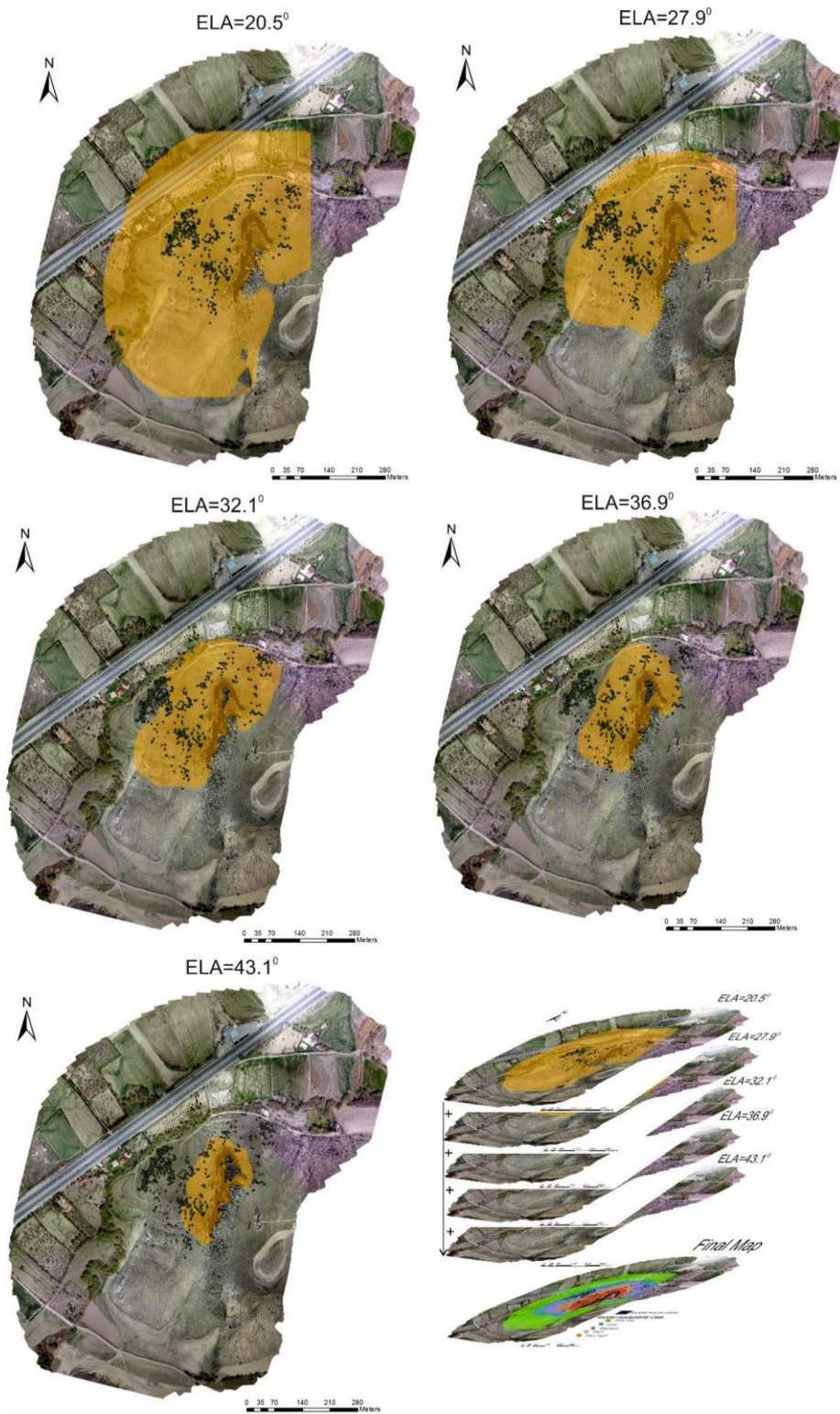


**Fig. 18** Rockfall propagation zones of the Kargabedir Hill rockfall area for each limit ELA values and combining them for a final map (from Kalender 2017)



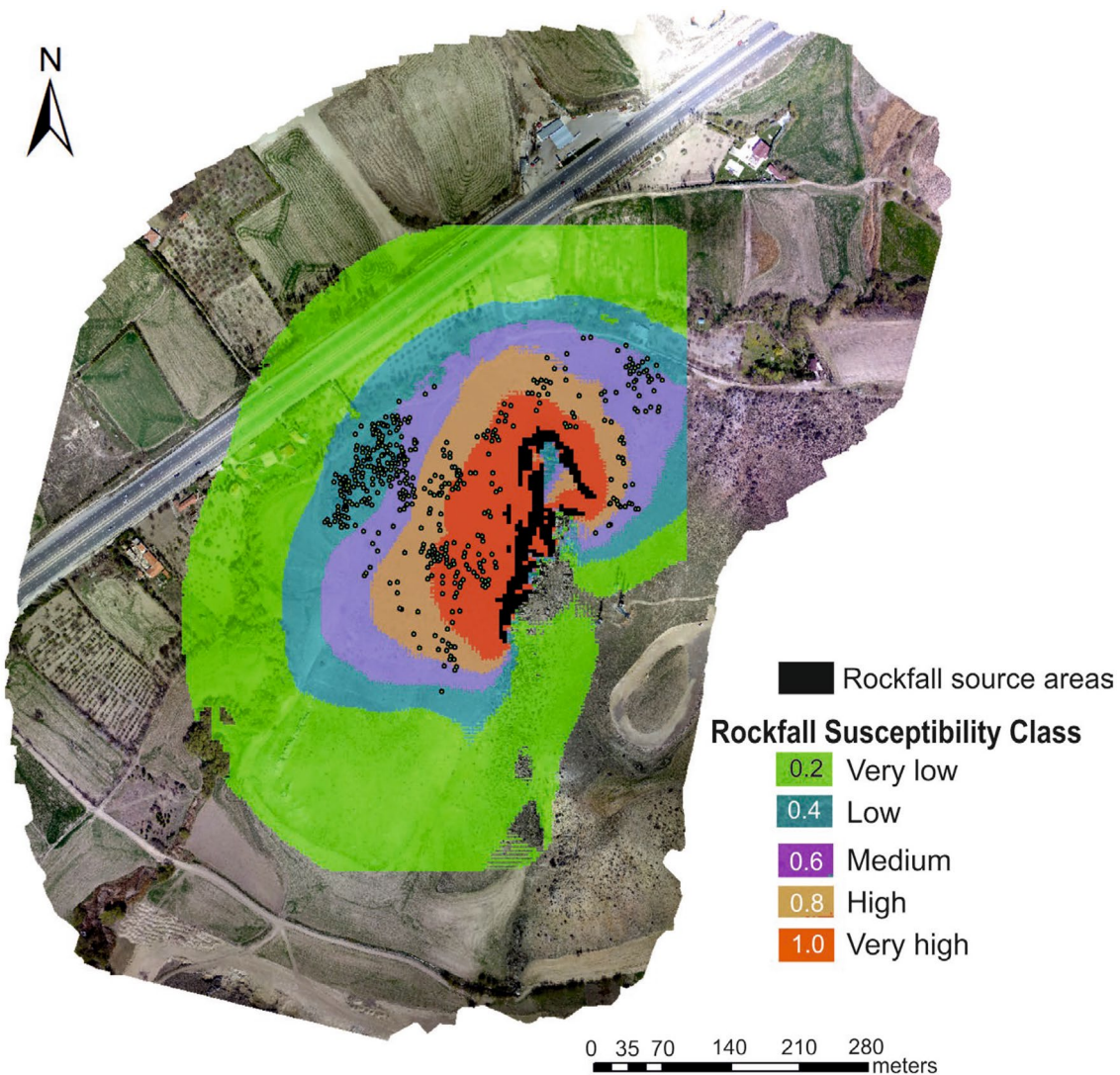


**Fig. 19** Rockfall susceptibility map of the Kargabedir Hill rockfall area (from Kalender 2017)

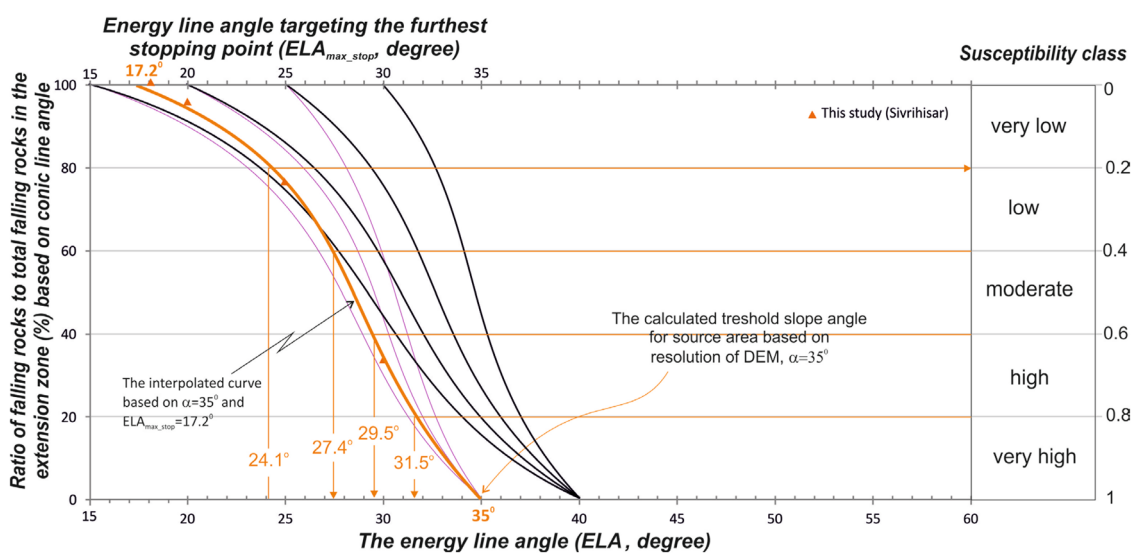


**Fig. 20** Determination of the susceptibility boundary ELA values for the Sivrihisar residential rockfall area from the interpolated curve (from Kalender 2017)

**Table 9** ELA ranges for susceptibility classes of Sivrihisar rockfall area (from Kalender 2017)

Susceptibility classes	Susceptibility values	ELA ranges for each susceptibility class (°)
None	0	<17.2
Very low	0.2	17.2–24.1
Low	0.4	24.1–27.4
Medium	0.6	27.4–29.5
High	0.8	29.5–31.5
Very high	1	>31.5

$$\Delta ELA = ELA_{\max\_stop} - \alpha \quad (4a)$$

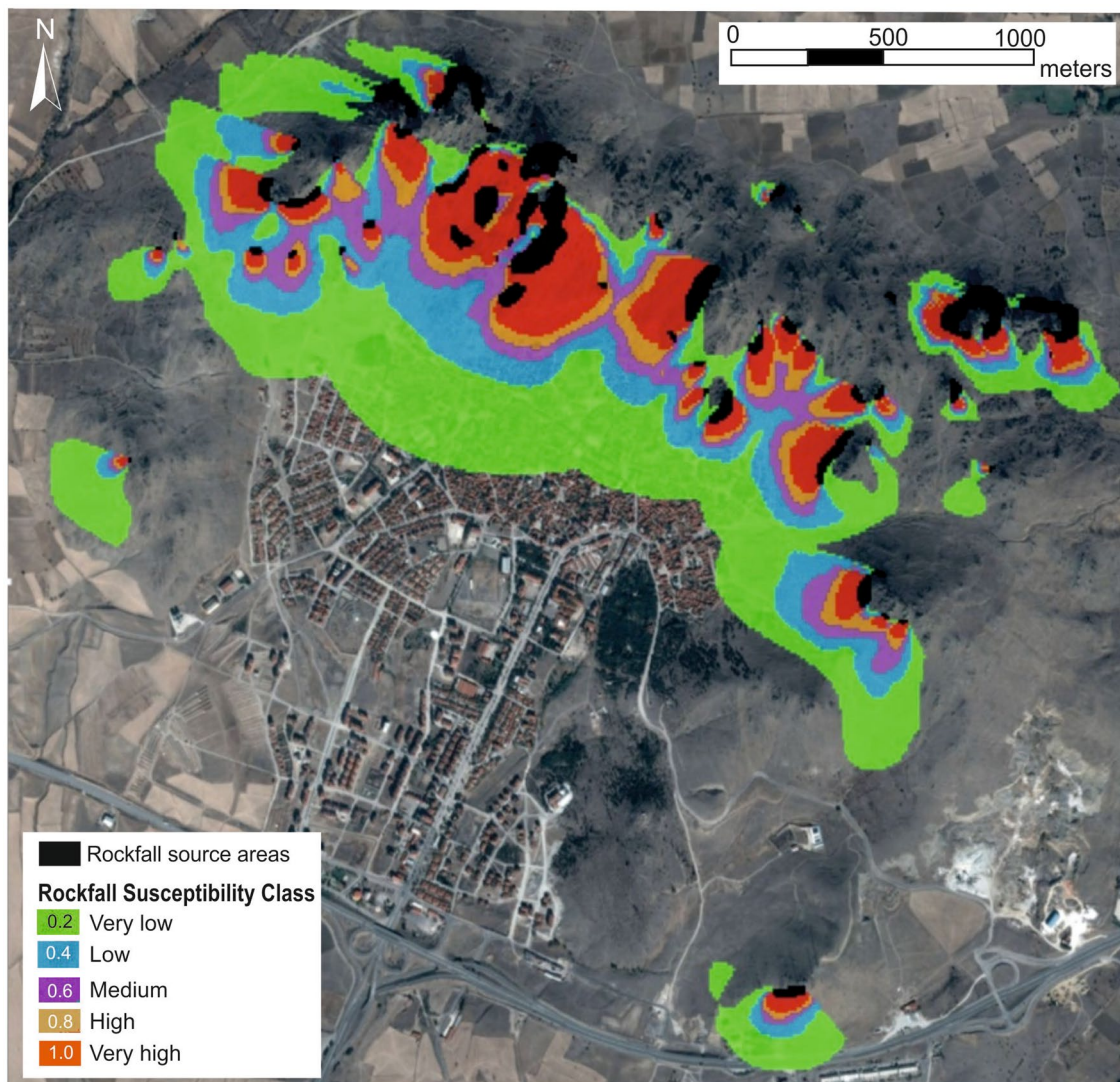
$$ELA' = \frac{5(ELA - ELA_{\max\_stop})}{\Delta ELA} \quad (4b)$$

$$P = 1 - \left( \frac{1.005}{1 + e^{-ELA'}} \right)^{2\pi} \quad (4c)$$

$$RS = 1 - P \text{ or } P = 1 - RS \quad (4d)$$

$$ELA' = -\ln \left( \frac{1.005}{((1 - P)^{1/2\pi})} - 1 \right) \quad (4e)$$

$$ELA = \frac{ELA' \times \Delta ELA}{5} + ELA_{\max\_stop} \quad (4f)$$

**Fig. 21** Rockfall susceptibility map of the Sivrihisar residential rockfall region on Google Earth view (from Kalender 2017)



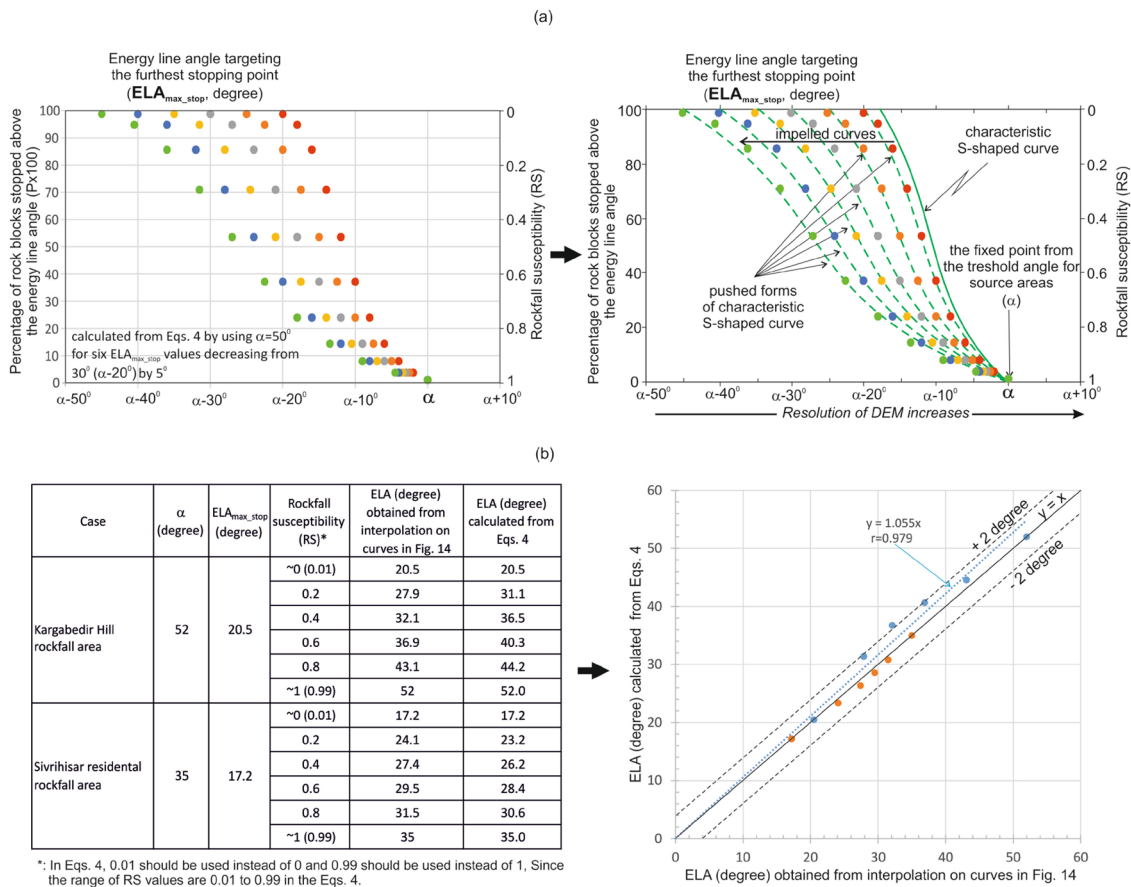


**Fig. 22** The performance of the developed equations on the original S-shaped curves was controlled by using the original curves given in Fig. 12, and the ELA values of two studied cases, namely Kargabedir Hill and Sivrihisar residential areas, were obtained from the original curves by interpolation based on the values of  $\alpha$  and  $ELA_{max\_stop}$

where RS varies between 0 and 1, ELA is the energy line angle in degrees for any RS value,  $\alpha$  is the threshold angle in degrees for source areas, and  $ELA_{max\_stop}$  is the energy line angle in degrees for targeting the maximum run-out distance. Only one issue should be taken into consideration, that is, 0.01 should be used instead of 0 and 0.99 should be used instead of 1, since the range of RS values is from 0.01 to 0.99 in Eqs. 4a–4f.

The performance of the developed equations on the original S-shaped curves was also controlled by using the original curves given in Fig. 12, and the ELA values of two studied cases, namely Kargabedir Hill and Sivrihisar residential area, were obtained from the original curves by interpolation based on the values of  $\alpha$  and  $ELA_{max\_stop}$  (Fig. 22). As seen in Fig. 22a, the calculated points from Eqs. 4a–4f are successfully overlapping on the curve given in Fig. 13 to which it belongs. In addition to the high performance of the developed equations on the curves given in Fig. 12, the cross-correlation between the ELA values of two studied cases obtained from the original curves by interpolation and the plotted values of ELA calculated by Eqs. 4a–4f for the same rockfall susceptibility boundaries such as very low, low, medium, high, and very high susceptibility classes were scattered very closely to the  $y = x$  line with a high correlation coefficient equal to 0.979 (Fig. 22b).

The derived equations produce very successful outputs compatible with the original S-shaped curves given in Fig. 13. Therefore, the developed equations have high potential particularly to be used in computer codes for the rockfall susceptibility mapping based on the cone propagation approach.

## Discussion and conclusions

In this study, an innovative methodology for the adjustable use of energy line angle for susceptibility mapping by using the cone propagation approach was proposed. The main considerations of the study, which should be underlined, were discussed and concluded as follows.

The limited number of well-studied rockfall data regarding the percentage of the fallen rock blocks stopped in the area bordered by an energy line angle was investigated in literature (see Fig. 2). When data belonging to Toppe (1987) was ignored, an S-shaped curvilinear relationship can be fitted for these well-studied data. In fact, the S-shaped curvilinear relationship statistically defines the cumulative normal statistical distribution curve of an event. In this study, two rockfall-prone cases, namely Kargabedir Hill and Sivrihisar residential regions, were studied for data collection. It is obviously seen that the S-shaped curves fitted to each data obtained

from four cases, two of which are our data from Turkey, in addition to cases by Onofri and Candian (1979) and Larcher et al. (2012), are different. In this study, by using an innovative approach, it was ensured that the four different S-shaped curves are represented by a characteristic S-shaped curve. Then, an adjustable energy line angle for susceptibility mapping by using the cone propagation approach was developed, considering the characteristic S-shaped curve. The use of characteristic S-shaped curve independent from region increases the applicability of the use of the proposed innovative approach to the other regions.

In this study, almost all possible S-shaped curves obtained for any rockfall-prone region were produced by impelling the characteristic S-shaped curve, considering the site-specific values of  $\alpha$  and  $ELA_{max\_stop}$  as the starting and ending points, respectively. In addition to the graphical presentations given in Fig. 13, a series of practical equations were also derived for the use of an adjustable energy line angle to be considered in susceptibility mapping by the cone propagation approach. The series of practical equations have high potential particularly when used in computer codes for the rockfall susceptibility mapping based on the cone propagation approach. After the innovative improvements on the cone propagation approach, it is possible to determine the energy line angles corresponding to rockfall susceptibility classes from the graphical (or equational) presentation of the S-shaped curve adjusted by considering the site-specific values of  $\alpha$  and  $ELA_{max\_stop}$ .

The innovative approach for the use of adjustable energy line angle for mapping different degrees of rockfall susceptibility zones in the propagation zone is the main subject of our study. On the other hand, an initial attempt was also included for determination of  $ELA_{max\_stop}$  in the final part of the study. The value of  $\alpha$  is closely sensitive to the resolution of the digital elevation model (DEM), and it is open to the user control in Geographic Information System (GIS) medium. However,  $ELA_{max\_stop}$ , which may have values in wider ranges, mainly depends on the properties of the rock blocks and the slope surface properties. However, as a good foothold to start our attempt, it is possible to mention the possible lowest and highest values of  $ELA_{max\_stop}$  based on a large number of studies in the literature. In this study, the lowest and highest values of  $ELA_{max\_stop}$  were selected as  $15^\circ$  and  $45^\circ$ , respectively. Of course, the practitioner can be preferred the use of  $15^\circ$  from the conservatively point of view; however, to be too conservative may not be economical in engineering perspective. The relationship between the lowest and highest values of  $ELA_{max\_stop}$  was associated by a rating system, namely RDR, that considers the rock blocks and slope surface properties. Furthermore, a reducing constant ( $\Delta$ ) was also included in the relations to ensure being on the safe side.

In this study, to relatively simplify the structure of the RDR system, the prominent parameters on the maximum run-out distance of rockfall events were taken into consideration. However, the preferred parameters in this study should not be interpreted as there are no other parameters that may be effective on run-out distance, because it should be taken into consideration that the RDR system is open to improvement. The determined value of  $ELA_{max\_stop}$  by using the proposed approach in this study is not an indispensable value; however, it can be taken into consideration as a preliminary default value open to user control. Due to the empirical structure of the methodology, the suggested supportive approach to the practitioners for determining  $ELA_{max\_stop}$  should be considered as an initial attempt with its flexibility to open improvement.

## Acknowledgements

The authors would like to thank Dr. Inan Ulusoy for providing and processing the data obtained from drone flights and also would like to present their special thanks to Prof. Dr. Murat Ercanoglu for sharing his knowledge about Geographic Information System (GIS) during the use of the ArcGIS software. In addition, the authors would like to thank Prof. Dr. Murat Ercanoglu for the calculation of the ELA values of the falling blocks in the Ankara Castle rockfall area based on the published study by Aksoy and Ercanoglu (2006). The authors sincerely appreciate Dr. Ioannis Farmakis and the anonymous reviewers for all their valuable comments and suggestions during the review process, which helped us to improve the quality of our paper.

## Author contribution

All authors contributed to the study conception and design. Material preparation and data collection and analysis were performed by Aycan Kalender and Harun Sonmez. The first draft of the manuscript was written by Aycan Kalender, and all authors commented on previous versions of the manuscript. All authors read and approved the final manuscript. This paper was prepared from the PhD thesis of Aycan Kalender who is listed as the principal author.

**Funding** Open access funding provided by the Scientific and Technological Research Council of Türkiye (TÜBİTAK).

## Data availability

The required data presentations sufficiently were given in the manuscript.

## Declarations

**Competing interests** The authors declare no competing interests.

**Open Access** This article is licensed under a Creative Commons Attribution 4.0 International License, which permits use, sharing, adaptation, distribution and reproduction in any medium or format, as long as you give appropriate credit to the original author(s) and the source, provide a link to the Creative Commons licence, and indicate if changes were made. The images or other third party material in this article are included in the article's Creative Commons licence, unless indicated otherwise in a credit line to the material. If material is not included in the article's Creative Commons licence and your intended use is not permitted by statutory regulation or exceeds the permitted use, you will need to obtain permission directly from the copyright holder. To view a copy of this licence, visit <http://creativecommons.org/licenses/by/4.0/>.

## References

- Agisoft PhotoScan (2017) Software version 1.3.0. <http://www.agisoft.com/>. Accessed 21 Apr 2017
- Aksoy H, Ercanoglu M (2006) Determination of the rockfall source in an urban settlement area by using a rule-based fuzzy evaluation. *Nat Hazards Earth Syst Sci* 6:941–954
- Antoniou AA, Efthimios Lekkas E (2010) Rockfall susceptibility map for Athinios port, Santorini Island, Greece. *Geomorphology* 118:152–166

- Corominas J, Copons R, Moya J, ilaplana, J.M., Altimir, J., Jordi Amigo, J. (2005) Quantitative assessment of the residual risk in a rockfall protected area. *Landslides* 2:343–357
- Crosta GB, Agliardi F (2003) A methodology for physically based rockfall hazard assessment. *Nat Hazards Earth Syst Sci* 3:407–422
- Crosta G, Frattini P, Sterlacchini S (2001) Valutazione e gestione del rischio da frana. Regione Lombardia, Milano, 169 pp
- Dorren LKA (2012) Rockyfor3D (v4.1) revealed – transparent description of the complete 3D rockfall model. *ecorisQ Pap.*, pp. 1–30
- Emre O, Duman T, Ozalpl S, Elmaci H, Olgun S, Saroğlu F (2013) Annotated active fault map of Turkey. General Directorate of Mineral Research and Exploration, Special Publication Series 30. Ankara, Türkiye
- Environmental Systems Research Institute, Inc. [ESRI] (2007) ArcGIS version 9.1. GIS Software, NewYork
- Evans S, Hungr O (1993) The assessment of rockfall hazard at the base of talus slopes. *Can Geotech J* 30:620–636
- Farmakis I, Marinos V, Papanthassiou G, Karantanellis E (2020) Automated 3D jointed rock mass structural analysis and characterization using LiDAR terrestrial laser scanner for rockfall susceptibility assessment: Perissa area case (Santorini). *Geotech Geol Eng* 38:3007–3024
- Farmakis I, DiFrancesco PM, Hutchinson DJ, Vlachopoulos N (2022) Rockfall detection using LiDAR and deep learning. *Eng Geol* 309:106836
- Farvacque M, Corona C, Lopez-Saez J, Mainieri R, Stoffel M, Bourrier F, Eckert N, David Toe D (2022) Estimating rockfall release frequency from blocks deposited in protection barriers, growth disturbances in trees, and trajectory simulations. *Landslides* 19:7–18
- Gerber W (1994) Beurteilung des Prozesses Steinschlag, Forstliche Arbeitsgruppe Naturgefahren (FAN). Herbstkurs Poschiavo, Kursunterlagen, WSL, Birmensdorf, 20 pp., (in German)
- Heim A (1932) *Der Bergsturz und Menschenleben*. Fretz und Wasmuth Verlag, Zürich, p 218
- Jaboyedoff M, Labiouse V (2003) Preliminary assessment of rockfall hazard based on GIS data. In: 10 International Congress on Rock Mechanics ISRM, pp. 575–578
- Jaboyedoff M, Labiouse V (2011) Technical note: Preliminary estimation of rockfall runoff zones. *Nat Hazards Earth Syst Sci* 11(3):819–828
- Jaboyedoff M, Oppikofer T, Abellan A, Derron MH, Loye A, Metzger R, Pedrazzini A (2012) Use of LIDAR in landslide investigations: a review. *Nat Hazards* 61:5–28
- Kalender A (2017) Investigations of relations between cone-fall angle and geologic and morphologic parameters on rockfall analyses. Hacettepe University Graduate School of Science and Engineering, PhD. Thesis (unpublished, in Turkish)
- Kalender A, Sonmez H (2019) Evaluation of rockfall susceptibility of Kargabedir Tepe (Ankara-Eskişehir Highway) region by cone propagation approach using unmanned aerial vehicle (UAV) images. *Journal of Geological Engineering* 43(2019):187–210
- Kromer RA, Rowe E, Hutchinson J, Lato M, Abellan A (2018) Rockfall risk management using a pre-failure deformation database. *Landslides* 15:847–858
- Lan H, Martin CD, Lim CH (2007) RockFall Analyst: a GIS extension for three-dimensional and spatially distributed rockfall hazard modelling. *Compt Rendus Geosci* 33:262–279
- Larcher V, Simoni S, Pasquazzo R, Strada C, Zampedri G, Berger F (2012) WP6 guidelines Rockfall and Forecast systems, Italy
- Lied K (1977) Rockfall problems in Norway. In: *Rockfall dynamics and protective work effectiveness*. ISMES, Bergamo, vol. 90, pp. 51–53
- Onofri R, Candian C (1979) Indagine sui limiti di massima invasione di blocchi rocciosi franati durante il sisma del Friuli del 1976, Reg. Aut. Friuli – Venezia Giulia, Cluet, 42 pp., (in Italian)
- Quanterra (2003) Conefall (v1.0) user's guide. Open report-Soft 01. Retrieved from [https://quanterra.ch/wp-content/uploads/2016/02/conefall\\_manual.pdf](https://quanterra.ch/wp-content/uploads/2016/02/conefall_manual.pdf)
- Ritchie AM (1963) Stability of rock slope vol 17. Highway Research Board, National Academy of Sciences-National Research Council., in *Evaluation of Rockfall and its Control*, pp. 13–28
- Rocscience Inc. (2017) Coefficient of restitution table, retrieved from <https://www.rocscience.com/help/rockfall/documentation/slope/materials/reference-tables/rocscience-coefficient-of-restitution-table-in-rockfall>. Access date to website: April 2017
- Rocscience Inc. (2023) Coefficient of restitution table, retrieved from <https://www.rocscience.com/help/rockfall/documentation/slope/materials/reference-tables/rocscience-coefficient-of-restitution-table-in-rockfall>. Access date to website: January 2023
- Rojay B, Suzen L (1997) Tectonostratigraphic evolution of the Cretaceous dynamic basins on accretionary ophiolitic melange prism SW of Ankara region. *TAPG Bulletin* 9(1):1–12
- Samodra G, Chen G, Sartohadi J, Hadmoko DS, Kasama K, Setiawan MA (2016) Rockfall susceptibility zoning based on back analysis of rockfall deposit inventory in Gunung Kelir, Java. *Technique Note, Landslides* 13:805–819
- Toppe R (1987) Terrain models — a tool for natural hazard mapping. *Proc Davos Symp Sept 1986(162):629–638*
- Varnes DJ (1978) Slope movements: types and processes. Transportation Research Board, Special Report No, Washington, DC, p 176
- Wieczorek GF, Morrissey MM, Iovine G, Godt J (1998) Rock-fall Hazards in the Yosemite Valley, California. USGS Open-file Report, pp. 98–467. <https://doi.org/10.3133/ofr98467>
- Williams JG, Rosser NJ, Hardy RJ, Brain MJ (2019) The importance of monitoring interval for rockfall magnitude-frequency estimation. *J Geophys Res Earth Surf* 124:2841–2853
- Yılmaz H (2003) Geochemical exploration for gold in western Turkey: success and failure. *J Geochem Explor* 80:117–135

---

**Aycan Kalender** (✉) · **Harun Sonmez**

Department of Geological Engineering, Applied Geology Division, Hacettepe University, 06800 Beytepe, Ankara, Turkey  
Email: aycancoskun@hacettepe.edu.tr